5268168

Sandia National Laboratories
Waste Isolation Pilot Plant

Analysis Report for: Testing of a Proposed BRAGFLO Grid to be used for the Compliance Recertification Application Performance Assessment Calculations

Author: Joshua Stein (6821)	Print	Joshua S. Stein	3/24/03
		Signature	Date
Author: William Zelinski (6821)	Print	William Zelinski	3/24/03
		Signature	Date
Technical Review: Cliff Hansen (6823)	Print	Clifford Hansen	3/24/03
		Signature	Date
Management Review: David Kessel (6821)	Print	David Kessel	3/24/03
		Signature	Date
QA Review: Mario Chavez (6820)	Print	Mario Chavez	3/24/03
		Signature	Date

© 2003 Sandia Corporation

WIPP:1.3.5.1.2.1:PA:QA-L:DPRP1:526587

Information Only

TABLE OF CONTENTS

Information Only

TABLE OF FIGURES

Information Only

Information Only

Information Only

Information Only

1 EXECUTIVE SUMMARY

This analysis report describes a set of BRAGFLO calculations presented to the Salado Flow Peer Review panel in February 2003 and described in the Technical Baseline Migration (TBM) BRAGFLO analysis report (Hansen et al., 2002). This panel first met in May 2002 to assess proposed changes to three conceptual models used in the Performance Assessment (PA) of the Waste Isolation Pilot Plant (WIPP). These original changes are described in an analysis report (Hansen et al., 2002) and in the first report of the peer review panel (Caporuscio et al., 2002). In response to the panel's first report, Sandia National Laboratories conducted an additional set of analyses, which are described in this report. These calculations incorporated several modifications to the conceptual model changes presented to the panel in May 2002.

These modifications to the May 2002 conceptual models (Hansen et al., 2002) include the incorporation of a simplified shaft seal model in the BRAGFLO grid, modeling fracturing in the upper and lower Disturbed Rock Zone (DRZ), and other minor changes and corrections described in the body of this report and in the corresponding analysis plan (Stein and Zelinski, 2003).

Pressure and saturation from BRAGFLO are compared to results from the Technical Baseline Migration (TBM) to assess whether these changes significantly affect BRAGFLO results and whether the complementary cumulative distribution functions (CCDFs) from the TBM are still a valid approximation of our current understanding of the WIPP PA. The comparison concluded that the effect of these changes on the BRAGFLO results are so minor that the results of a total system PA using these new results would be essentially identical to the total system PA results of the TBM (Dunagan, 2003).

The comparisons show that only minor differences in pressures and saturations arise from these changes. In the vast majority of vectors pressures and saturations are nearly equivalent to the TBM. This equivalence is especially evident in the plots of average pressures and saturations for all vectors. In certain rare cases there are significant differences between individual vectors. These differences occur in only a few vectors. There are several reasons for these differences. Saturation in the waste panel following a brine pocket intrusion is especially sensitive to pressure changes if the pressure in the brine pocket and repository are nearly equal, as is the case in several vectors. Also vectors with pressures above the fracturing initiation pressure are very sensitive to small pressure changes because of the exponential link between pressure and permeability in the fractured materials. In both of these rare cases, brine flow into the waste panels, either from the borehole or from the DRZ and Marker Beds, can be quite sensitive to small differences in repository pressures. Despite the few vectors that display differences, the great majority of vectors behave nearly the same as in the TBM calculation.

In addition to running BRAGFLO we also calculated the spallings CCDF from the AP106 BRAGFLO results and compared it to the TBM spallings CCDF. There

Information Only

are no significant differences between the results. Since cuttings and cavings releases are not affected by BRAGFLO results, and since the combination of cuttings, cavings, and spallings accounts for more than 99% of the total releases, it is evident that the TBM CCDFs remain a valid approximation of our current understanding of WIPP performance assessment.

In addition, we ran a single undisturbed scenario in which we adjusted the pore volume of the upper and lower DRZ in the southern half of the waste filled repository to simulate one effect of raising this part of the repository up 2.4 m to Clay Seam "G". We compared the pressure and saturation results from these runs to the results of the AP106 runs described above. The most significant differences are minor variations in saturation that are expected due to the change in the pore volume of the DRZ, but none of the differences could significantly change release calculations. Since these changes to the DRZ pore volume did not significantly affect BRAGFLO results it is not necessary to include an explicit representation of the change in repository horizon for the BRAGFLO calculations supporting the Compliance Recertification Application.

2 INTRODUCTION AND OBJECTIVES

In May 2002, the Salado Flow Peer Review panel met in Carlsbad to evaluate changes to conceptual models for the performance Assessment (PA) of the Waste Isolation Pilot Plant (WIPP). These changes are detailed in a report by Hansen et al. (2002). To demonstrate the effects of these changes on BRAGFLO results a set of PA calculations (The Technical Baseline Migration (TBM)) was run. The peer review panel judged the changes to be "generally sound in their structure, reasonableness, and relationship to the original models," however the panel required that a total systems PA be run and complementary cumulative distribution functions (CCDFs) be generated before they would agree to the changes (Caporuscio et al., 2002). In response to this finding, Sandia National Laboratories (SNL) has run a total system PA for the TBM and produced CCDFs (Dunagan, 2003) that were presented to the Salado Flow Peer Review panel during their second and last meeting in Carlsbad in February 2003.

After the initial meeting of the Salado Peer Review panel in May 2002, the U.S. Department of Energy (DOE) received two letters from the Environmental Protection Agency (EPA) (EPA, 2002a; 2002b) with a list of topics that EPA would like to be considered by in the PA calculations for the Compliance Recertification Application (CRA). Additional issues and concerns were discussed in a series of technical exchange meetings with the EPA. Two of the topics considered in these meetings relate specifically to assumptions made for the TBM BRAGFLO calculations: (1) the presence or absence of the shaft in the BRAGFLO model grid, and (2) the move of the repository horizon up approximately 2 m to Clay Seam "G" for panels 3, 4, 5, 6, and 9. These panels are located in the southern half of the waste disposal area.

Information Only

2.1 Simplified Shaft

The TBM calculations did not include an explicit model of the shaft seal system in the BRAGFLO grid. The shaft was removed because in all the previous calculations no significant flow occurred in this region and the shaft model required that nearly 1,000 separate parameters be defined. In subsequent discussions, SNL was led to believe that the presence of the shaft in the grid was considered to be important by EPA. Therefore SNL presented to EPA an approach for implementing a simplified shaft model with equivalent properties to the original detailed model. This work is described in AP-094 (James and Stein, 2002) and in the associated analysis report (James and Stein, 2003).

2.2 Clay Seam "G"

The second issue relates to a request by DOE to EPA to raise the repository horizon in panels 3, 4, 5, 6, and 9 so that the roof is at Clay Seam "G" (DOE, 2000). EPA responded to the request in a letter (EPA, 2000) in which EPA agreed with DOE that the effects to long-term performance would be minimal. At the time, SNL considered the change minor enough not to warrant a full-scale impact assessment. However, in a subsequent letter from EPA the Agency indicated that "the conceptual model of the repository should reflect the change to raise the level of excavation to Clay Seam G. The conceptual change should be appropriately addressed in the modeling, if warranted" (EPA, 2002a). In response to this letter, SNL began an effort to evaluate the effects, if any, on PA resulting from the move in the repository horizon. Specifically, SNL initiated two sets of analyses:

1. The horizon change may influence the creep-closure porosity surface calculated by the code SANTOS and used by BRAGFLO. The SANTOS calculations are being repeated with the new horizon to test whether the response surface will change significantly. This work is in progress and is described in AP-093 (Park, 2002).

2. The thickness of upper and lower Disturbed Rock Zone (DRZ) represented in the BRAGFLO grid may change due to the horizon change. This change may affect flow pathways around the Option D panel closures as well as the total pore volume represented in the DRZ above and below the waste rooms. A new BRAGFLO grid was developed to include these changes and two sets of BRAGFLO simulations were run to test whether these changes significantly affect WIPP PA. This analysis report describes the results of this work, which was outlined in Analysis Plan AP106 (Stein and Zelinski, 2003).

Information Only

3 APPROACH

This report summarizes the results of BRAGFLO and a limited set of CCDFGF results which were presented to the Salado Flow Peer Review panel during the February, 2003 meetings. For these meetings we ran two sets of analyses. In the first set we ran a full replicate consisting of five BRAGFLO scenarios (S1-S5) using a modified version of the TBM BRAGFLO grid, which hereafter we will refer to as the CRA grid because the Salado Flow Peer Review panel has approved of its use for that purpose. We had initially only planned to run three scenarios (S1, S3, and S5) and compare pressure and saturation results to the TBM to see if there were any significant differences caused by the changes (Stein and Zelinski, 2003). However, based on wishes expressed by the peer review panel members, we ran two additional scenarios (S2 and S4) so that we could calculate the spallings CCDF and directly compare it to the TBM results (Dunagan, 2003). The aim of this first set of analyses was to test if whether modifications and corrections made the TBM conceptual models significantly affected BRAGFLO and other PA results. These modifications include: addition of the simplified shaft, allowing fracturing in the upper DRZ, and correcting minor errors found in the TBM. The approach and results of this first set of calculations will be presented first.

In the second set of analyses, we ran a variation of the undisturbed scenario (S1) in which we "adjusted" DRZ porosity to evaluate the significance of the reduced pore volume in the upper DRZ and the increased pore volume in the lower DRZ in the half of the repository raised to Clay Seam "G". The aim of these runs was to test whether an explicit representative of the raised repository is necessary for PA calculations. The results of these "variation" runs are compared to the results from the first set of runs in the final section of this report.

3.1 CRA Grid

The CRA grid is described below in detail. It is essentially the TBM grid with the following changes:

1. The simplified shaft model was included in the grid.
2. Double-wide panel closures in north end.
3. Modifications to allow fracture flow "around" the Option D panel closures both above and below the closure concrete through the DRZ and marker beds were made.
4. A minor error relating to the volume of the rest of the repository regions in the TBM grid (Stein, 2002) was corrected.

The CRA grid used in this analysis is shown as a logical grid in Figure 1. For comparison, the TBM grid is shown in Figure 2.

Information Only

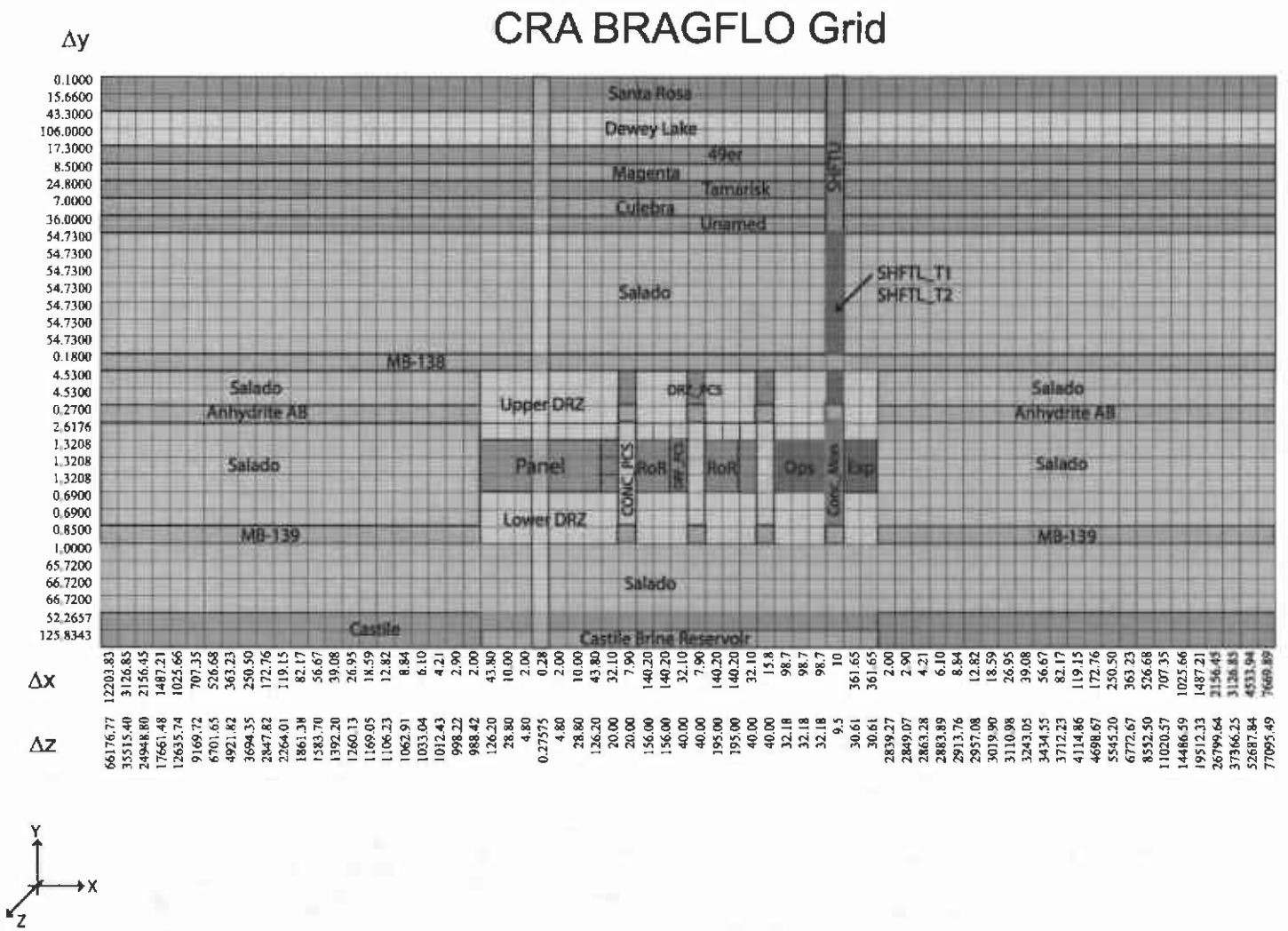

Figure 1. The Compliance Recertification Application (CRA) logical BRAGFLO grid.

Information Only

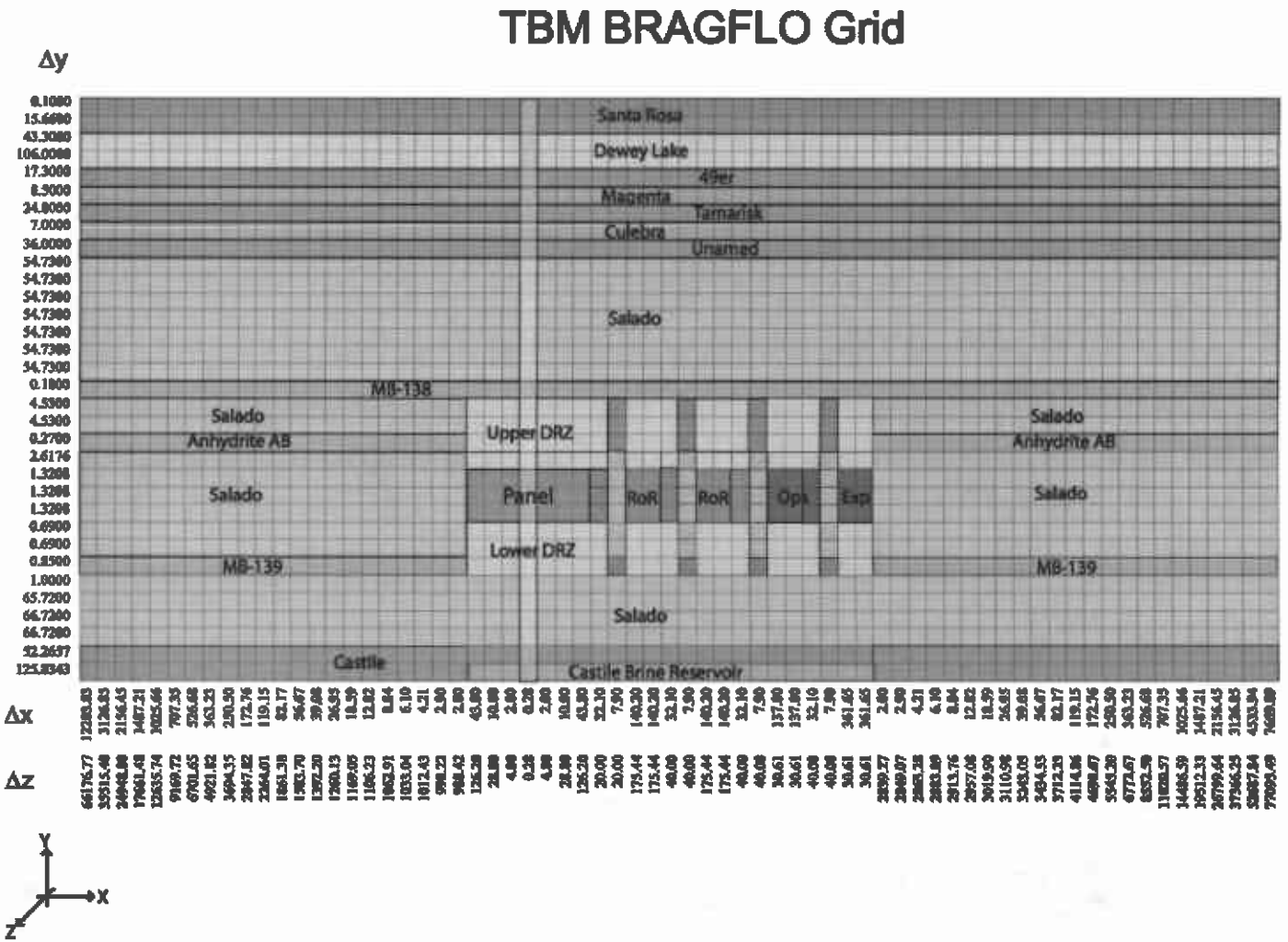

Figure 2. Technical Baseline Migration (TBM) logical BRAGFLO grid.

Information Only

3.2 Simplified Shaft Model

A shaft seal model is included in the CRA grid but it is implemented in a simpler fashion to that used for the CCA and PAVT. A detailed description of the model and its parameters are discussed in AP-094 (James and Stein, 2002) and the resulting analysis report (James and Stein, 2003). The new model does not alter the conceptual model of the shaft seal components as described in SNL (1996). Rather, it conservatively represents the behavior of seal components in the repository system model. Specifically, the original 11 separate material layers that defined the shaft model for the CCA will be reduced to two layers each with properties equivalent to the composite effect of the original materials combined in series. Additionally, the six time intervals that were used to represent the evolution of the shaft seal materials over time are reduced to two intervals.

3.3 Double Wide Panel Closure Concrete in North End of Repository

In the TBM grid, an Option D panel closure was included between the operations area and the experimental area. In the CRA grid, the bottom of the simplified shaft that is represented by the material CONC_MON replaced this panel closure. This material is the same that was used for the bottom of the original shaft model implemented in the CCA and PAVT calculations. To account for this panel closure that is immediately south of the shaft, the dimensions of the concrete portion of the panel closure located between the northern rest of repository and the operations area was doubled (7.9 m x 2 = 15.8 m). This ensures that gas produced in the waste regions must effectively travel though the same number of panel closures to reach the experimental area as was modeled in the TBM. This is an important part of the revised conceptual model of repository geometry that was presented to the Salado Flow Peer Review panel.

3.4 Conceptual Model of DRZ Fracture

In the TBM conceptualization of the DRZ, the permeability and porosity in the DRZ were represented as they were for the PAVT. However, SNL determined that fracturing should not be allowed in the DRZ above the repository and therefore did not apply the fracturing model to this region of the grid. The upper DRZ was allowed to fracture in the PAVT in order to provide a gas path in the case of unrealistically high repository pressures. The PAVT analysis did not find unrealistic pressures in the repository; hence Sandia determined that the upper DRZ fracturing was not necessary for the TBM analysis since a fracture path was available in the lower DRZ. The argument made for allowing the lower DRZ to fracture was as follows. There is only a 1.4 m section of Salado halite between the repository floor and MB 139. As rooms close the floor heaves and fractures, and in the presence of higher gas pressures, fractures are not expected to heal thereby maintaining a hydraulic connection to MB 139. For this reason, fracturing was allowed only in the DRZ *below* the repository.

Information Only

3.4.1 Revision to the TBM Conceptual Model of DRZ Fracture

The proposed move of the repository horizon up 2.4 meters to Clay Seam "G" has led to a reevaluation of hydrofracture studies conducted in the WIPP underground in salt (Wawersik and Stone, 1989) and requires, that the assumptions about allowing (or not allowing) fracturing in the grid elements representing the DRZ, be modified from the conceptual model presented for the TBM (Hansen et al., 2002). Specifically, given the results of the hydrofracture studies and considering the variable permeability assigned to the DRZ, it is now justified to allow fracturing to occur in both the upper and lower DRZ. The move to Clay Seam "G" clarified the need for this change but even in the half of the repository,which is not raised, the proposed modification is still appropriate.

Figure 3 compares the raised and unraised repository configurations in relation to the surrounding stratigraphy. Specifically, in the raised half of the repository, the distance through the lower DRZ from the repository floor downward to MB 139 will increase from 1.4 m to approximately 3.8 m. This change means that fracturing associated with floor heave will likely be reduced in this part of the repository.

The raised waste rooms will have ready access to the Anhydrite "B" layer which will now be excavated to define the ceilings for the raised waste rooms. Anhydrite "B" is a thin (~6 cm-thick), layer that is present directly above Clay Seam G. In the event of high repository pressures it is just as likely that a fracture pathway might form (1) parallel to the roof of the repository via Anhydrite "B", (2) vertically through the 2 m-thick DRZ to Anhydrite "A", (3) perhaps all the way to MB 138 or, 3.8 m into the floor to MB 139.

The results of hydraulic fracturing tests performed in WIPP salt, 3-100 meters from excavated rooms (Wawersik and Stone, 1989), indicate that the pressures at which hydraulic fracturing is initiated, fall in a similar range as for hydrofracture tests done in anhydrite Marker Beds 139 and 140 (Wawersik et al., 1997). Fracture initiation pressures for the anhydrite tests ranged from 7.36 to 12.46 MPa with an average initiation pressure of 10.5 MPa. For comparison, the fracture initiation pressures for the salt tests ranged from 4.14 to 17.24 MPa with an average initiation pressure of 11.98 MPa (Wawersik and Stone, 1989). One important difference in the fracture behavior of intact salt is that because it is so impermeable, fractures in WIPP salt will tend to stop at more permeable anhydrite marker beds and change direction, moving along the bed rather than fracturing across beds (Wawersik et al., 1997). These data indicate that fractures in both materials will typically initiate at pressures below lithostatic and thus repository pressures significantly above lithostatic are unjustified and unexpected.

Because the data support the application of the fracture model to intact salt in addition to the Marker Beds, we allow fracturing in both the upper and lower DRZ in this analysis. Even in the parts of the repository that are not being raised to Clay Seam "G", the test results support implementing the fracture model to both the upper and lower DRZ, considering the inherent uncertainty in exactly how the system will

Information Only

behave under possible near-lithostatic stresses. The important process that the fracture model simulates is the bleed off of very high pressures. Whether these pressures will bleed off through the upper or lower DRZ is not known and therefore we allow it to go in either direction and let the model determine which way is more favorable under the specific conditions in each vector. The parameters used by the BRAGFLO fracture model and applied to the Marker Beds materials and the DRZ are justified, because they do not allow repository pressures to significantly exceed lithostatic pressure.

3.4.2 Interaction between DRZ and Option D Panel Closures

In the CRA grid, we represent regions where the Option D panel closures and the shaft intersect a Marker Bed as isolated blocks of marker bed material. This representation is warranted for two reasons.

1. First, the marker bed material has a very similar permeability distribution (10^{-21} to $10^{-17.1}$ m^2) as the concrete portion of the Option D panel closures ($10^{-20.699}$ to 10^{-17} m^2), and thus, assigning this material as anhydrite marker bed in the model has essentially the same effect as calling it concrete as long as pressures are below the fracture initiation pressure.

2. Second, in the case of high pressures (near lithostatic) it is expected that fracturing may occur in the anhydrite marker beds and flow could go "around" the panel closures out of the 2-D plane considered in the model grid. In this case the flow would be through the marker bed material that is already allowed to fracture. Therefore, assigning these isolated cells as anhydrite marker bed materials is appropriate.

Information Only

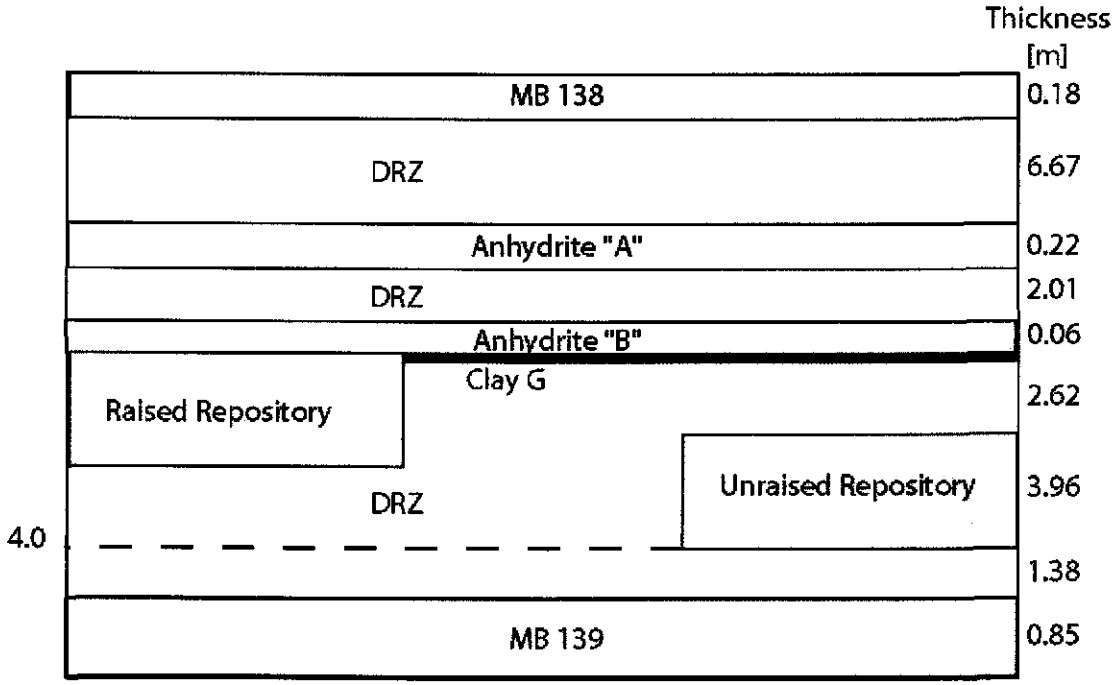

Figure 3. Schematic of the stratigraphy surrounding the raised and unraised sections of the repository. Not to scale.

3.5 Minor repository volume error corrected

A minor error in the dimensions of the TBM grid was identified during the calculations and documented by Stein in a memo to M.K. Knowles (Stein, 2002). Fixing this error required adjusting the delta Z dimensions of the rest of repository blocks. This was done for the CRA grid.

4 RESULTS PART 1

The AP106 BRAGFLO runs, completed as part of this analysis, used the same LHS random seed as was used for the TBM (Hansen et al., 2002). Therefore we can compare the results of these analyses on a vector-by-vector basis. As in the TBM BRAGFLO analysis, such a comparison is easily made by plotting the values of a single output variable at a single output time for all 100 vectors from two calculations (TBM and AP106, in this case) on a scatter plot. If the values of the output variable are nearly identical in both calculations, the 100 points will fall on the 1:1 line on the scatter plot. If there are differences between the results of the calculations, the points will lie off the 1:1 line. The sources of these differences can then be investigated more thoroughly with plots of time vs. output variable for specific vectors.

Information Only

The most important output variables in BRAGFLO are pressures and brine saturations in the waste regions, because these variables can significantly affect direct releases or radionuclides which are calculated by other codes in the Total Systems PA. For instance, the number of intrusions that result in a spallings release is a direct function of the pressure in the waste regions at the time of intrusion, which is calculated by BRAGFLO. Direct brine release (DBR) is an indirect function of repository pressure and brine saturation. The relation is indirect because a number of sampled variables other than pressure and saturation are also important in determining the magnitude of a DBR release, namely borehole permeability (Helton et al., 1998). Because pressure and saturation are the only BRAGFLO output variables that affect direct releases, we are focusing the analysis to comparisons of these variables. In addition, we include an analysis of flow in the simplified shaft to examine how the effectiveness of the simplified shaft model compares to original shaft seal model used in the CCA and PAVT.

This analysis will only examine three scenarios (S1, S3, and S5) in detail, because these scenarios cover the full range of expected conditions and the other scenarios will exhibit similar responses and are run primarily for the purpose of generating CCDF results.

All BRAGFLO output variables were interpolated to common times by the program SUMMARIZE. If changes in output variables are gradual such interpolation is quite accurate. An important exception to this includes processes immediately following a drilling intrusion when, for example, changes in borehole saturation can be quite rapid and variable, as brine may tend to flow toward the repository while gas flows away. Such highly transient flows can become obscured by the interpolation. However, since BRAGFLO runs do not have identical time-steps, interpolation is necessary for comparing results between different vectors and calculations. In most cases, this interpolation is very accurate. We will note when this is not the case.

4.1 Repository Pressures

Volume averaged pressures are calculated for important regions of the modeled repository. For this analysis we will focus on the variables: WAS_PRES and REP_PRES, the volume-averaged pressure in the single waste panel and the rest of repository (north and south combined), respectively. We have chosen representative times based on scenario to compare results of the AP106 runs with the TBM. Table 1 lists the times examined for each scenario.

Table 1. Times for which pressure and brine saturation results were analyzed in detail.

Scenario	Times
S1	1,000; 5,000; and 10,000 years
S3	2,000 and 10,000 years
S5	2,000 and 10,000 years

Information Only

4.1.1 S1 Pressures

Figure 4 shows average pressure in the waste panel (WAS_PRES) for all 100 vectors in the S1 scenario for the AP106 and TBM calculations. Average pressures tend to be somewhat higher in AP106 than TBM. This difference is caused by the replacement of one of the panel closures with the shaft seal model and the associated doubling of the concrete portion of the panel closure between the northern rest of repository and the operations area. In the TBM, gas from the waste panels had to traverse a single-wide panel closure in order to access the operations area whereas in the AP106 runs gas has to traverse a double-wide panel closure. This increase in the resistance to gas movement has the effect of slowing the movement of gas out of the waste regions, which causes slightly higher pressures over time. Although it is not clear in figure 4, the difference in pressure between the two calculations decreases with time. Figures 5-7 compare waste panel pressures for all vectors at the times specified in Table 1 and show that the pressure differences are most apparent at 1,000 years and less apparent at 5,000 and 10,000 years. Pressure differences decrease with time because gas generation does not continue at a constant rate. Gas generation is faster at early times, for two reasons: (1) early in the simulations repository pressures are lower and more brine enters the waste regions allowing gas generation to proceed at faster, inundated rates, and (2) most vectors with microbial gas production (50% of vectors) consume the available cellulosics, plastics, and rubbers in less than 1,000 years, after which microbial action does not generate any gas. Vector-by-vector differences are minor in all cases and are caused by the differences in the material property assignments in the different calculations.

Figure 8 shows the average pressure in the rest of repository (REP_PRES) for all 100 vectors in the S1 scenario for the AP106 and TBM calculations. Figures 9-11 compare rest of repository pressures for all vectors at the times specified in Table 1. The pressure differences between the AP106 and the TBM are somewhat less than were shown for the waste panel in figures 4-7, but the relative differences are similar, with AP106 having higher pressures than TBM. This is consistent with the double-wide panel closure retarding gas flow out of the waste regions. The differences are less because there are fewer panel closures between the rest of repository and the operation area to impede gas flow.

Information Only

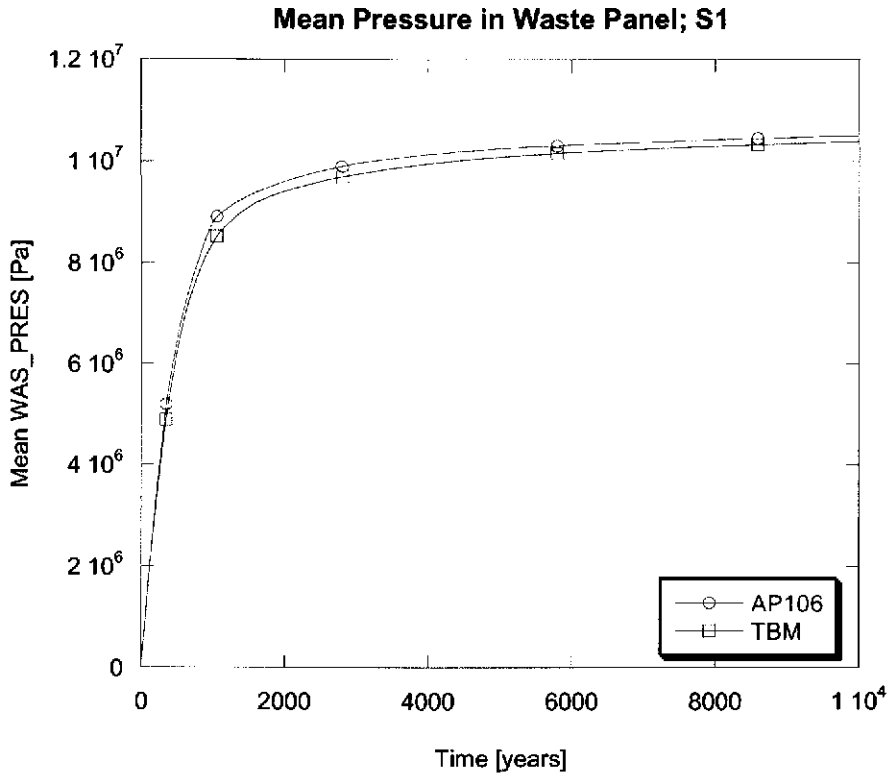

Figure 4. Average pressure in the waste panel for the AP106 and TBM S1 scenario.

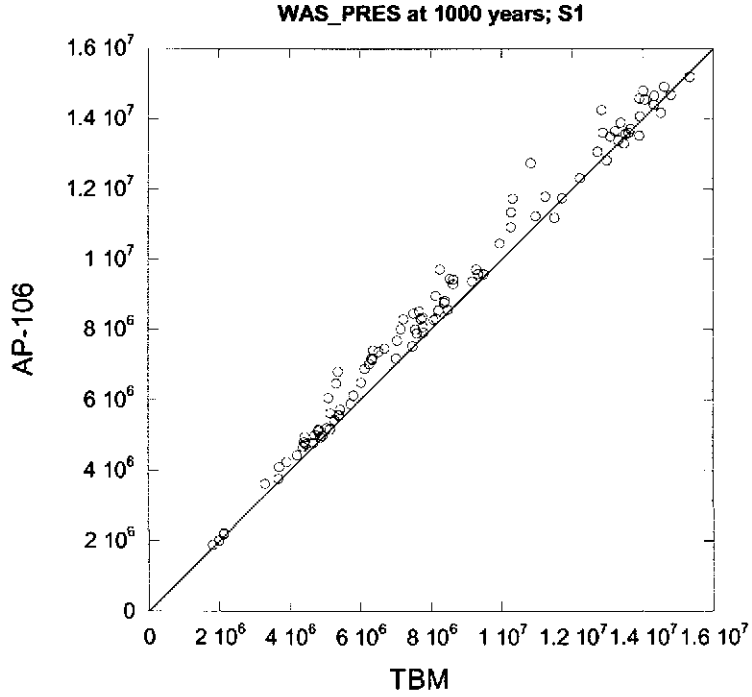

Figure 5. Scatter plot of pressure in the single waste panel at 1,000 years; S1

Information Only

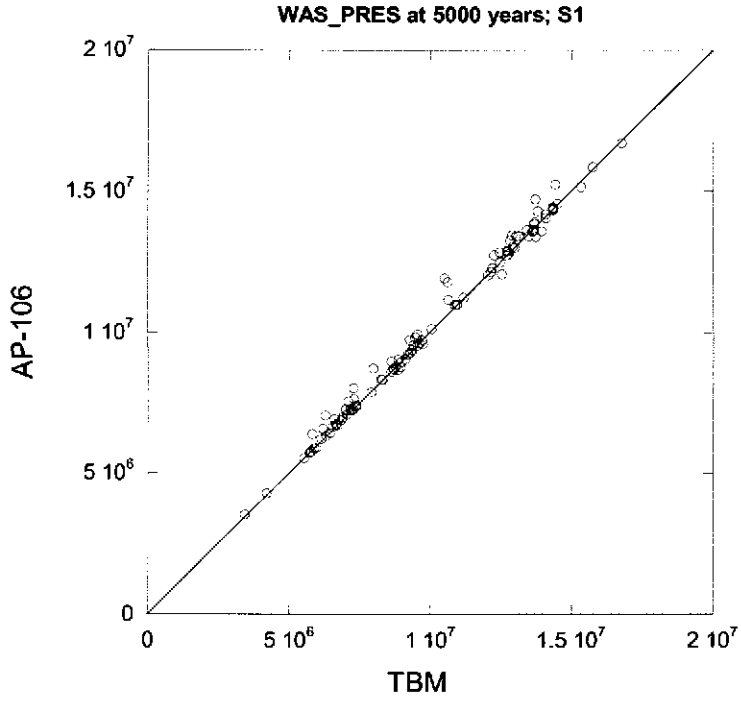

Figure 6. Scatter plot of pressure in the single waste panel at 5,000 years; S1

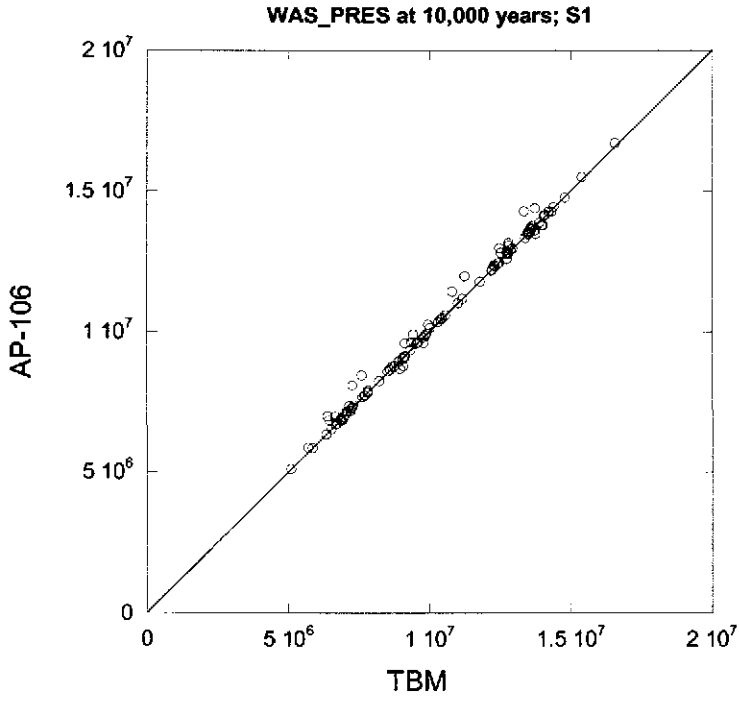

Figure 7. Scatter plot of pressure in the single waste panel at 10,000 years; S1

Information Only

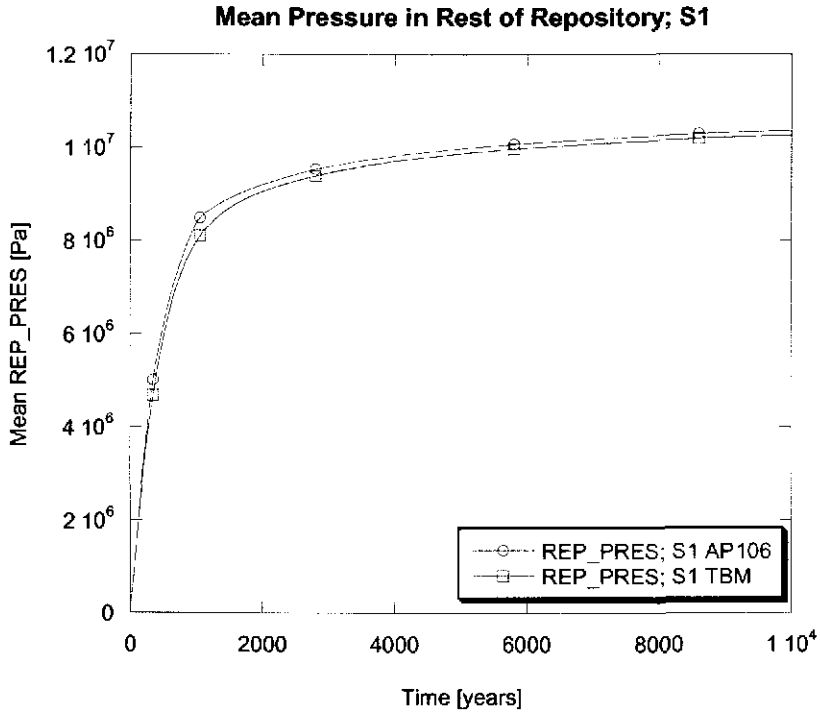

Figure 8. Average pressure in the rest of repository for the AP106 and TBM S1 scenario.

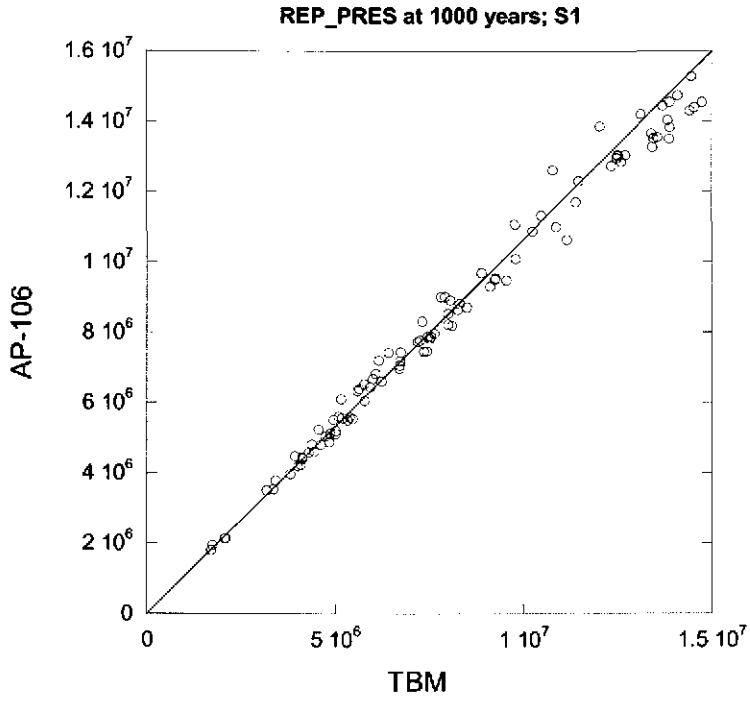

Figure 9. Scatter plot of pressure in the rest of repository at 1,000 years; S1

Information Only

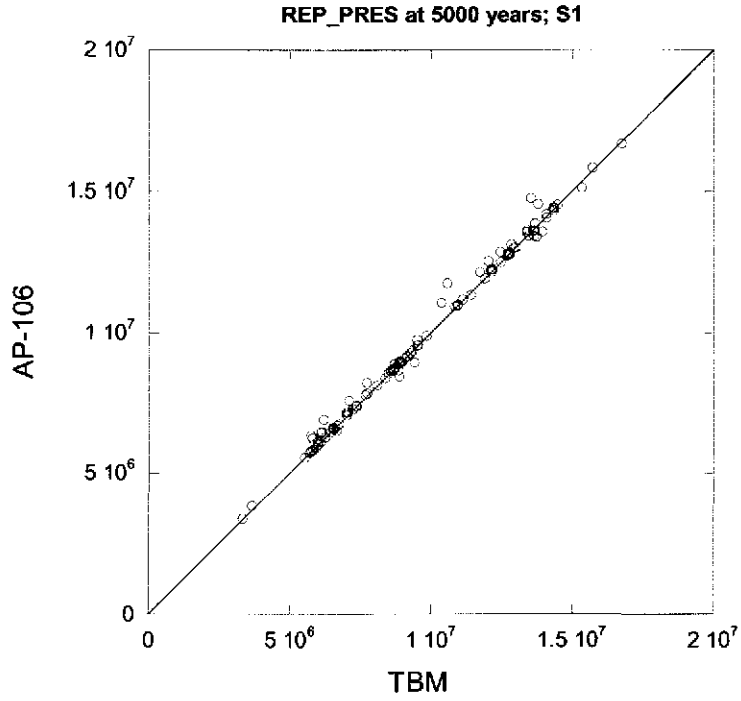

Figure 10. Scatter plot of pressure in the rest of repository at 5,000 years; S1

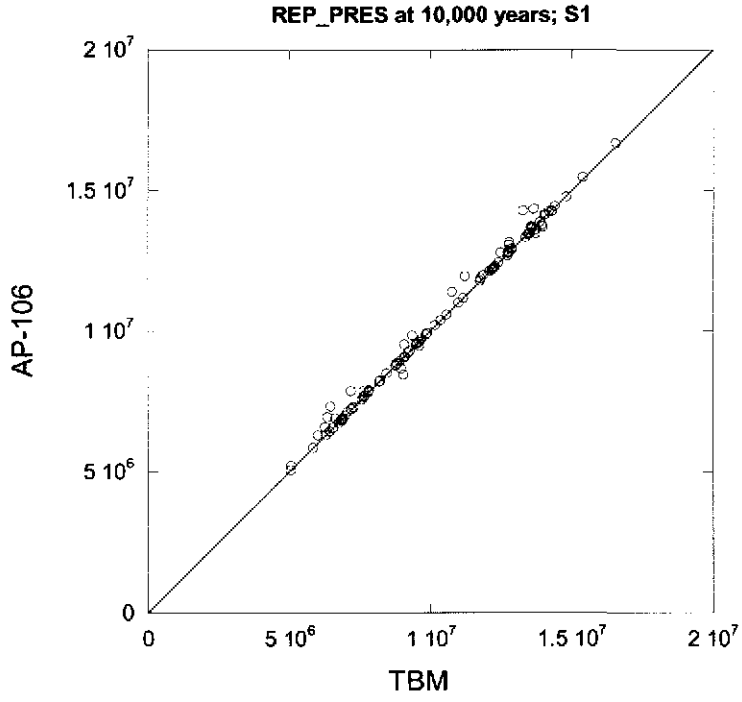

Figure 11. Scatter plot of pressure in the rest of repository at 10,000 years; S1

Information Only

4.1.2 S3 Pressures

Figure 12 shows average pressure in the waste panel (WAS_PRES) for all 100 vectors in the S3 scenario for the AP106 and TBM calculations. Average pressures tend to be nearly equal in AP106 and TBM in the waste panel indicating that the grid changes do not seem to affect repository pressures after an intrusion. This is because pressures in the waste panel following an intrusion are more sensitive to interactions with the brine pocket and the surface through the borehole than to the presence of the double-wide panel closures in the north. Figures 13 and 14 show scatter plots of WAS_PRES at 2,000 and 10,000 years. Vector-by-vector differences are minor in all cases further supporting the minimal effects of the grid changes.

Figure 15 shows average pressure in the rest of repository (REP_PRES) for all 100 vectors in the S3 scenario for the AP106 and TBM calculations. Average pressures in this region tend to be slightly greater in AP106 than in TBM. This difference is likely caused by the presence of the double-wide panel closure which impedes gas flow to the north. The effect of the double-wide panel closure is not seen in the intruded panel because in this scenario that region is connected directly to the brine pocket and the surface through the borehole. Figures 16 and 17 show scatter plots of REP_PRES at 2,000 and 10,000 years. Vector-by-vector differences are minor except for the significant outlier in figure 17.

The outlier is vector 87 and a detailed plot of pressure and brine saturation for this vector is shown in figure 18. This vector has high enough pressures at the time of intrusion that the DRZ is fracturing. In the TBM the pressure in the rest of repository gradually decreases with time following the intrusion as the high pressures bleed off either toward the intruded panel or toward the operations and experimental areas. After the intrusion the saturation in the rest of repository decreases to essentially zero, causing gas generation to cease. In AP106 the upper DRZ can fracture which causes an interesting effect in vector 87. Because the upper DRZ is fracturing, brine can continue to flow into the rest of repository through the upper DRZ causing gas generation to continue to nearly 6,000 years. This brine flow eventually stops causing the saturation to go to zero and then the pressures decrease as in the TBM, but this decrease is significantly delayed, causing vector 87 to appear as an outlier in figure 17.

Information Only

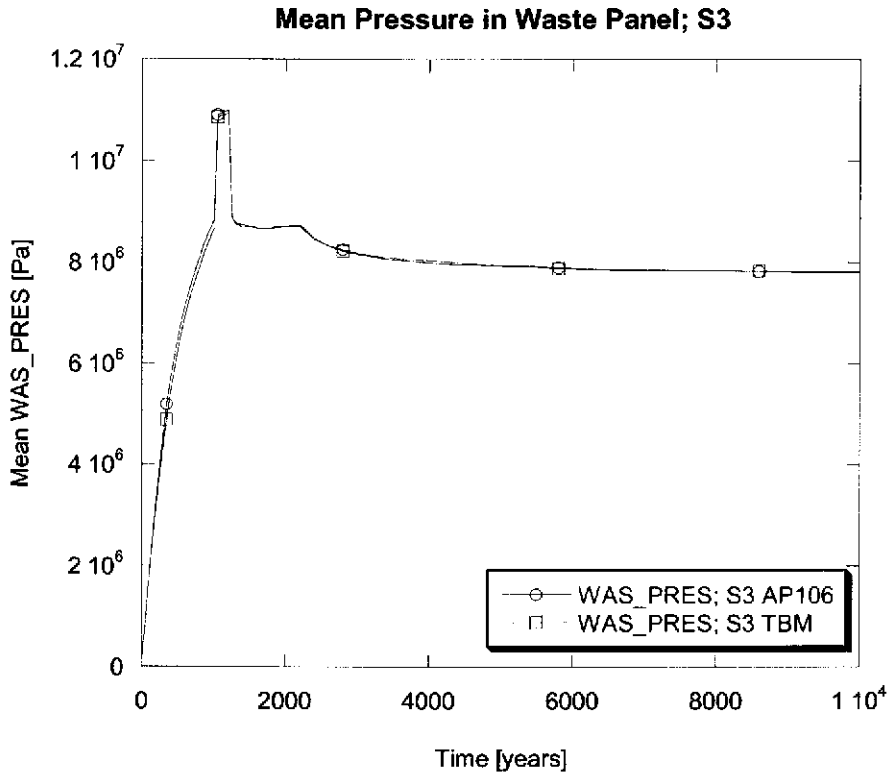

Figure 12. Average pressure in the waste panel for the AP106 and TBM S3 scenario.

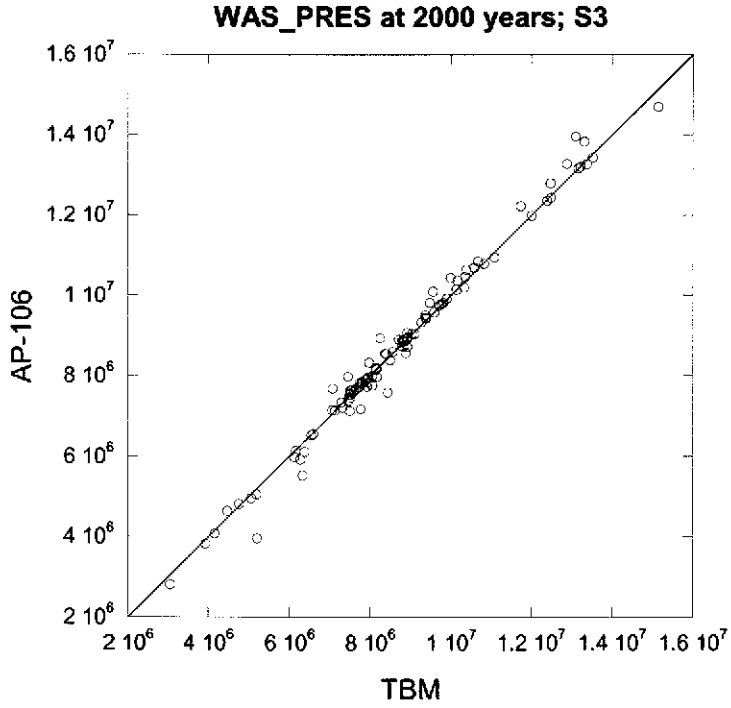

Figure 13. Scatter plot of pressure in the intruded panel at 2,000 years; S3

Information Only

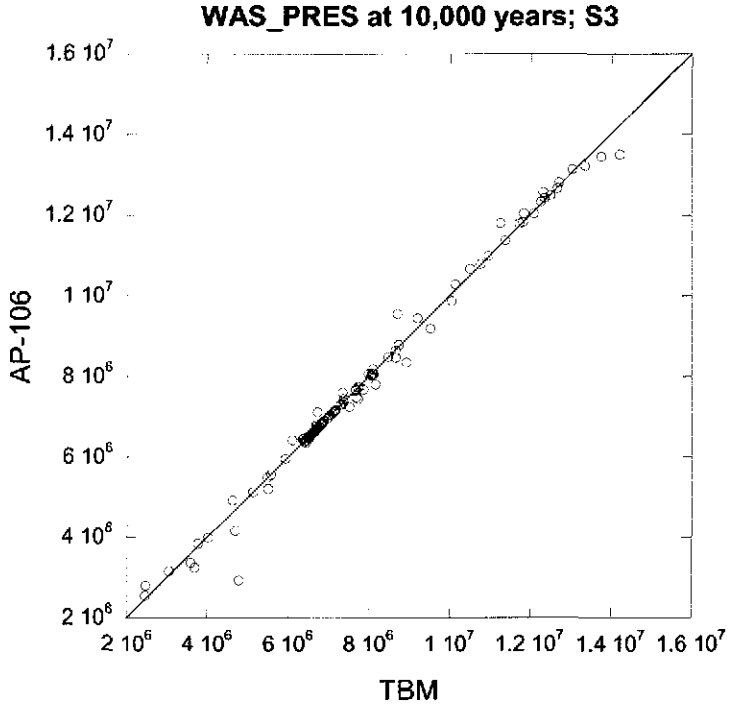

Figure 14. Scatter plot of pressure in the intruded panel at 10,000 years; S3

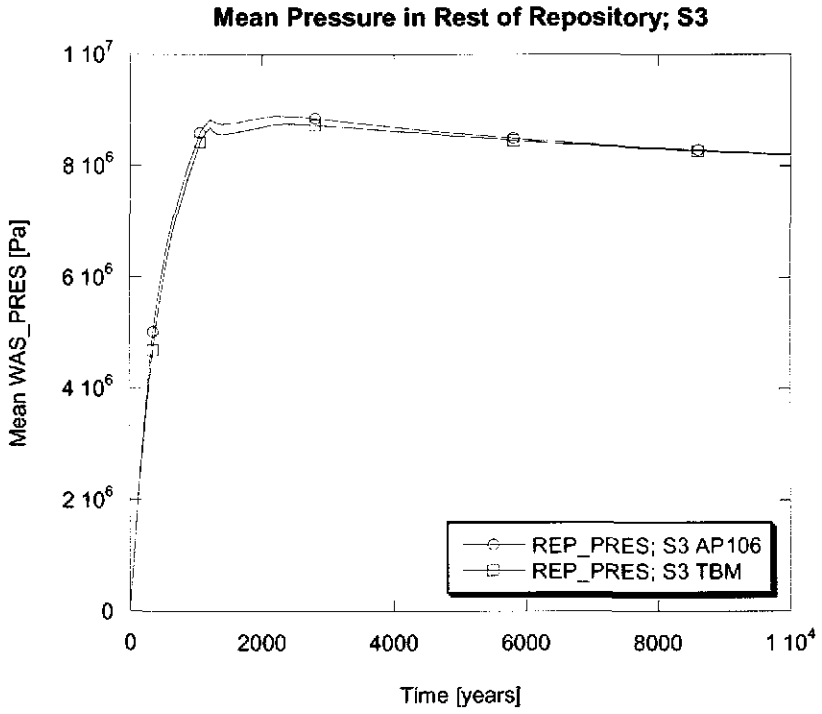

Figure 15. Average pressure in the rest of repository for the AP106 and TBM S3 scenario.

Information Only

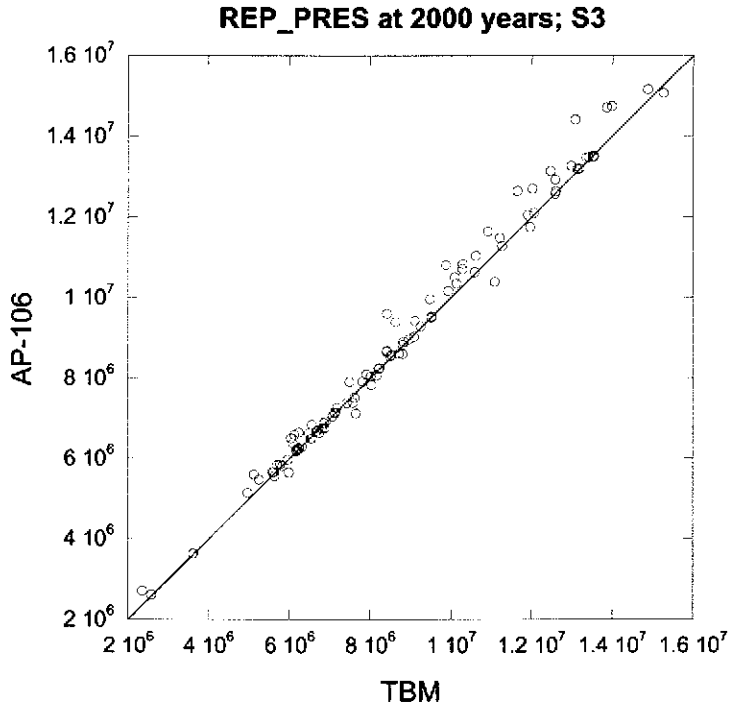

Figure 16. Scatter plot of pressure in the rest of repository at 2,000 years; S3

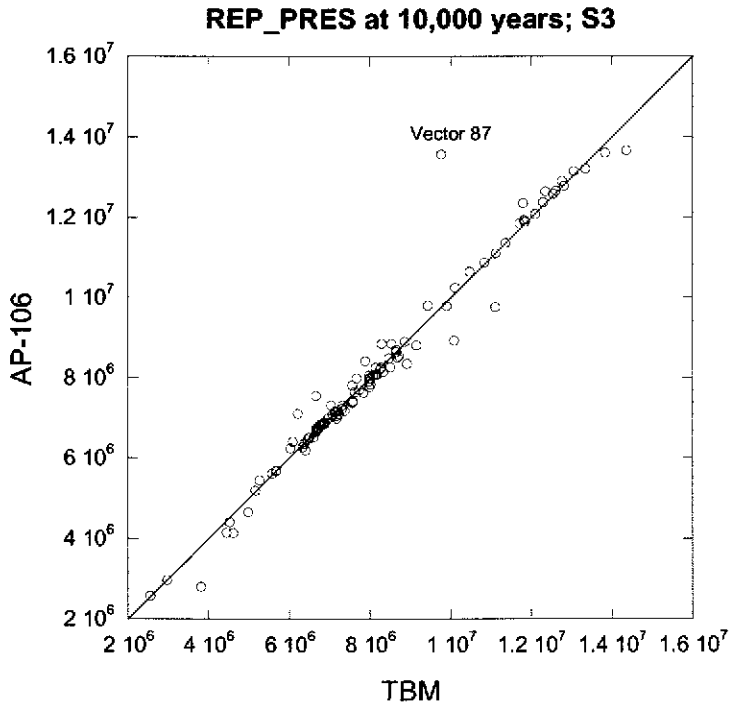

Figure 17. Scatter plot of pressure in the rest of repository at 10,000 years; S3

Information Only

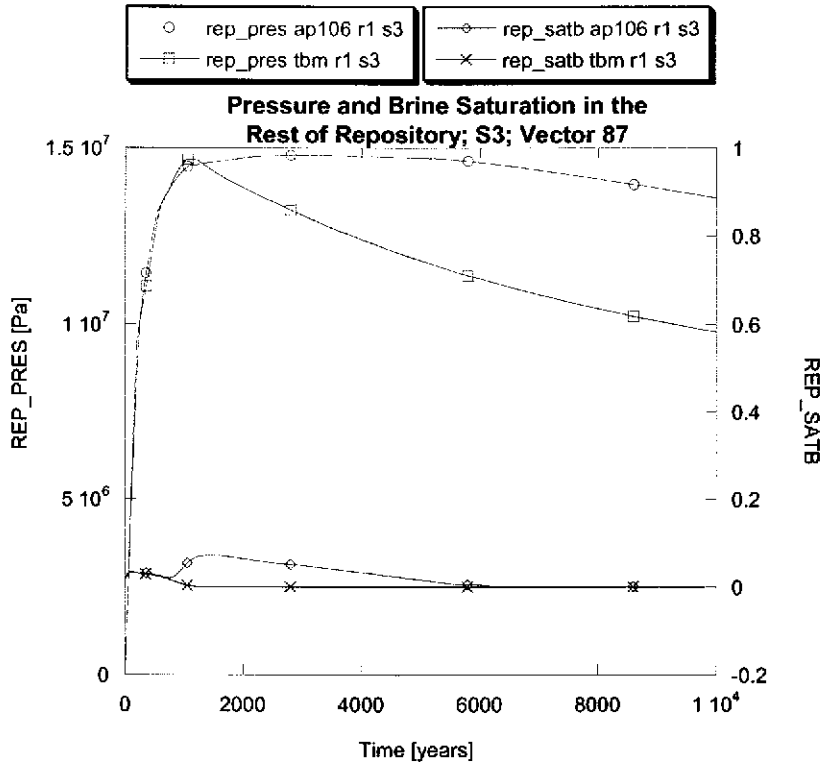

Figure 18. Detailed plot of pressure and brine saturation time histories for vector 87; S3

4.1.3 S5 Pressures

Figure 19 shows average pressure in the waste panel (WAS_PRES) for all 100 vectors in the S5 scenario for the AP106 and TBM calculations. Average pressures tend to be somewhat higher in AP106 than TBM. Figures 20 and 21 show scatter plots of WAS_PRES at 2,000 and 10,000 years. Vector-by-vector differences are minor in all cases.

Figure 22 shows average pressure in the rest of repository (REP_PRES) for all 100 vectors in the S5 scenario for the AP106 and TBM calculations. Average pressures in this region tend to somewhat greater in AP106 than in TBM. This behavior is consistent with the rest of repository being separated from the intruded panel by an Option D panel closure. This separation causes the rest of repository to behave in a similar manner as the rest of repository in the undisturbed scenario. Figures 23 and 24 show scatter plots of REP_PRES at 2,000 and 10,000 years. Vector-by-vector differences are minor except for the significant outlier in figure 24. This outlier is vector 87. We investigated the reason for the difference and found it to be the same reason as described for S3 pressures. In fact, the pressure and saturation plot for this vector looks nearly identical to figure 18.

Information Only

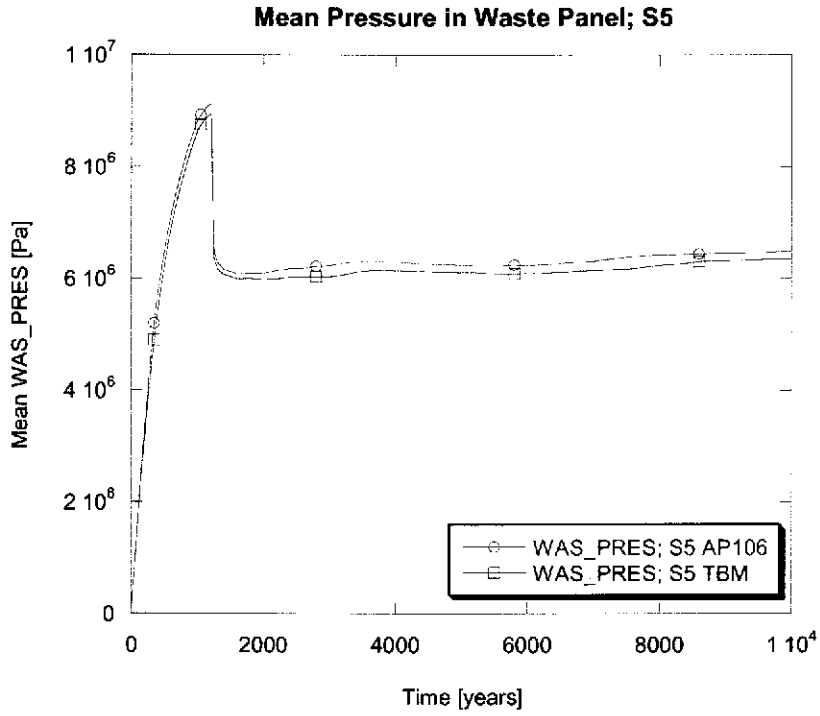

Figure 19. Average pressure in the waste panel for the AP106 and TBM S5 scenario.

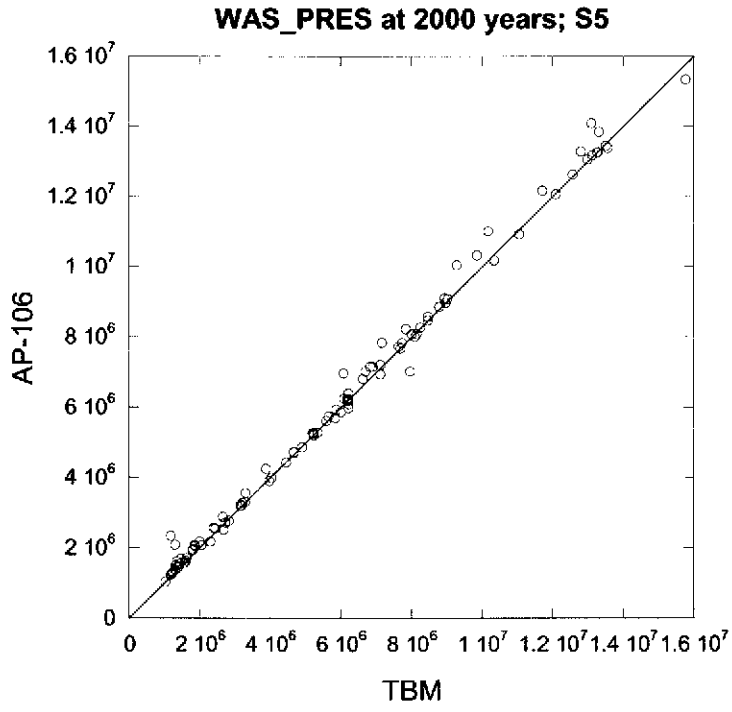

Figure 20. Scatter plot of pressure in the intruded panel at 2,000 years; S5

Information Only

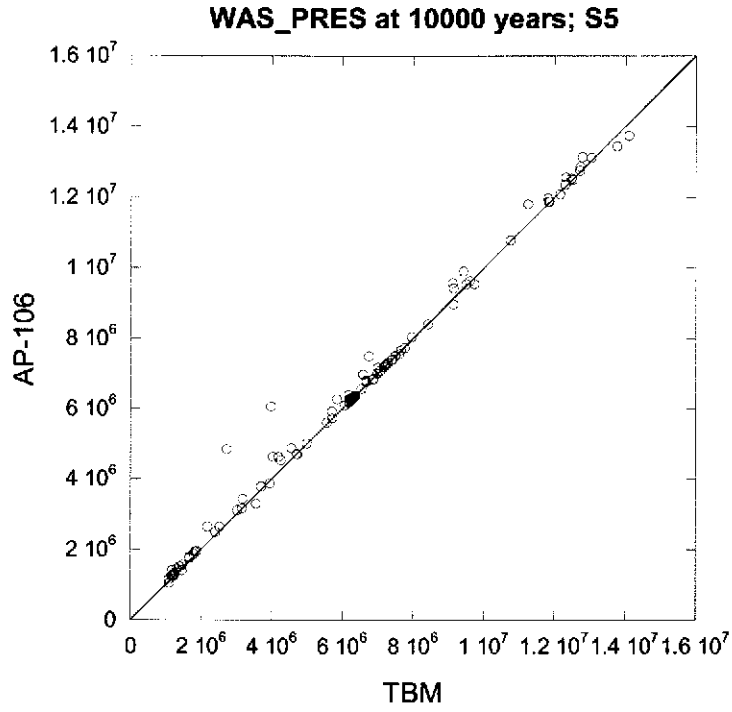

Figure 21. Scatter plot of pressure in the intruded panel at 10,000 years; S5

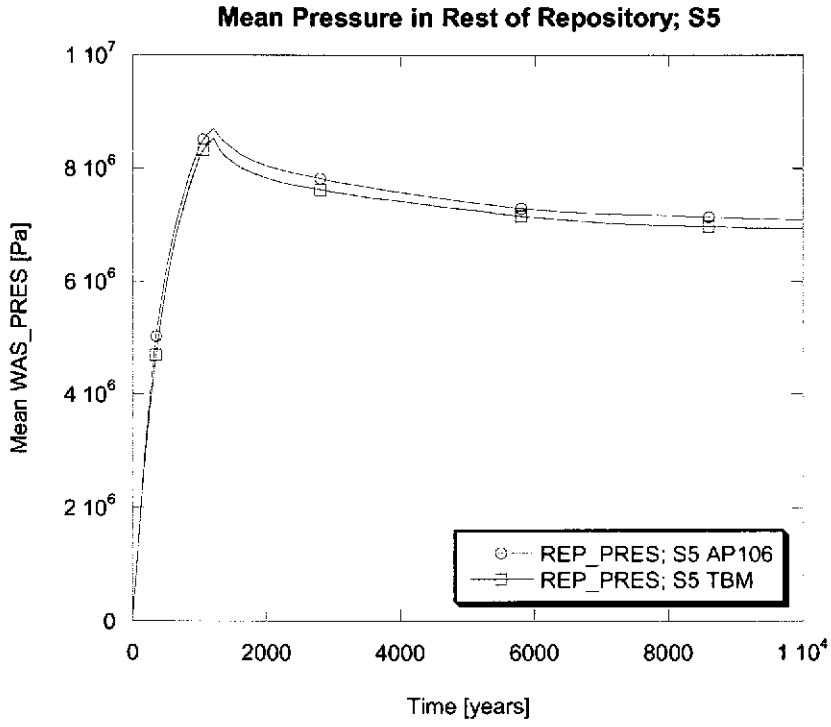

Figure 22. Average pressure in the rest of repository for the AP106 and TBM S1 scenario.

Information Only

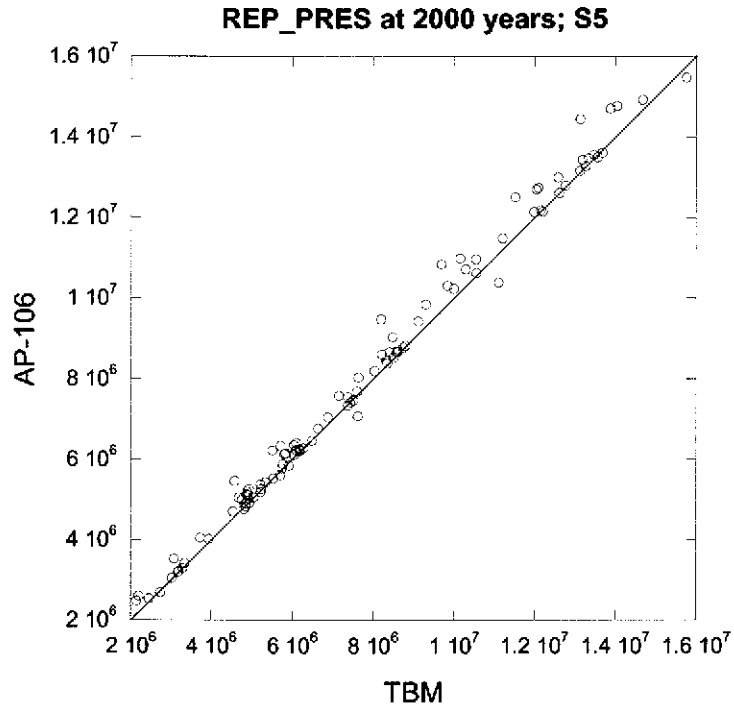

Figure 23. Scatter plot of pressure in the rest of repository at 2,000 years; S5

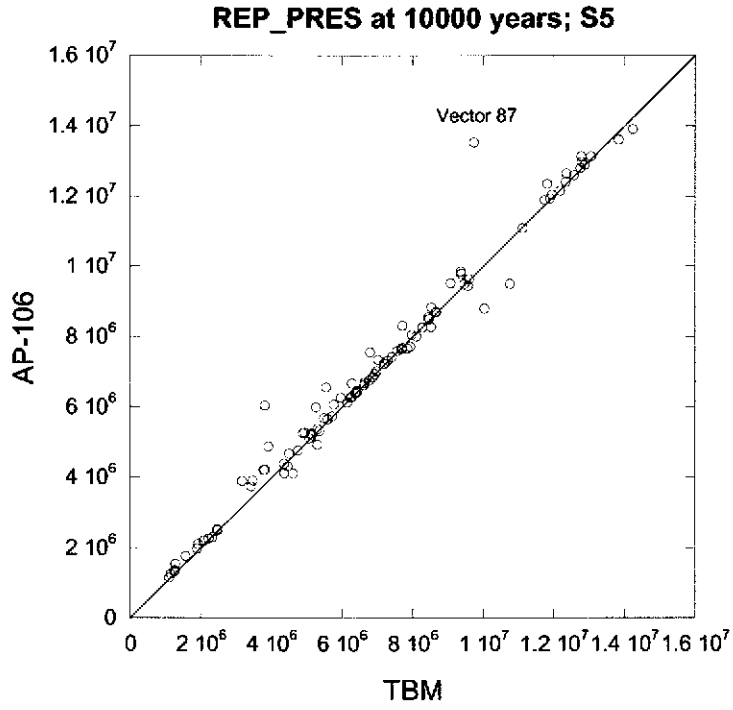

Figure 24. Scatter plot of pressure in the rest of repository at 10,000 years; S5

Information Only

4.2 Brine Saturations

Volume averaged brine saturations are calculated for important regions of the modeled repository. For this analysis we will focus on the variables: WAS_SATB and REP_SATB, the volume-averaged brine saturation in the single waste panel and the rest of repository (north and south combined), respectively. We have chosen the same representative times for the vector-by-vector comparisons as presented in Table 1.

4.2.1 S1 Brine Saturations

Figure 25 shows the average brine saturation in the waste panel (WAS_SATB) for all 100 vectors in the S1 scenario for the AP106 and TBM calculations. Average brine saturation is slightly higher in AP106 than TBM. Figures 26, 27 and 28 show scatter plots of WAS_SATB at 1,000; 5,000; and 10,000 years. Vector-by-vector differences are minor in all cases with vectors 28 and 58 showing the greatest differences. Figures 29 and 30 show detailed time histories of pressure and saturation for these vectors. Both of these vectors have high enough pressures that the DRZ is fracturing within several hundred years of the repository closing. Because fracturing in the upper DRZ is only implemented in AP106 this is the likely cause of differences.

Vector 28 shows that at about 4,000 years saturation rapidly increases in the waste panel in both calculations (Figure 29). Despite differences in the exact time when saturation changes begin both calculations display very similar patterns of saturation vs. time. AP106 displays higher saturations than the TBM after approximately 5,000 years. This is probably due to the fracturing in the upper DRZ in AP106, which results in higher permeabilities and greater potential for brine inflow from this area.

Vector 58 helps to illustrate how fracturing in the upper DRZ can affect pressure and saturation results in certain vectors. As soon as the pressures level out in vector 58, AP106 and TBM pressures cross each other several times as one calculation has slightly higher pressures than the other and vise versa. The calculation that tends to have higher pressures also tends to have lower saturations. This occurs, because higher pressures tend to push brine into the formation and the anhydrite beds, causing the brine saturation in the waste regions to decrease. Brine is immobile at saturations below residual saturation and can then only be consumed by corrosion reactions, which generate more gas and drive pressures higher. Because vector 58 is fracturing, slight pressure differences result in significant permeability changes in the fractured DRZ and anhydrite beds. When DRZ permeability rises more brine can flow into the waste areas increasing saturation. At first pressures in AP106 are higher because of the double-wide panel closure in the north end (see section 4.1.1). However this higher pressure causes the permeability in the upper DRZ to increase and gas is able to bleed off. This slight decrease in pressure allows more brine to

Information Only

enter the waste areas from the anhydrite beds and DRZ. Additional brine drives the gas generation reactions to produce more gas, which results in AP106 reaching higher pressures at about 2,000 years. At about 2,500 years the TBM begins to have more brine enter the waste rooms while the AP106 has consumed nearly all of the brine in the waste region via corrosion.

Figure 31 shows the average brine saturation in the rest of repository (REP_SATB) for all 100 vectors in the S1 scenario for the AP106 and TBM calculations. Average brine saturation is slightly higher in AP106 than TBM. Figures 32, 33 and 34 show scatter plots of REP_SATB at 1,000; 5,000; and 10,000 years, respectively. Vector-by-vector differences are minor in all cases.

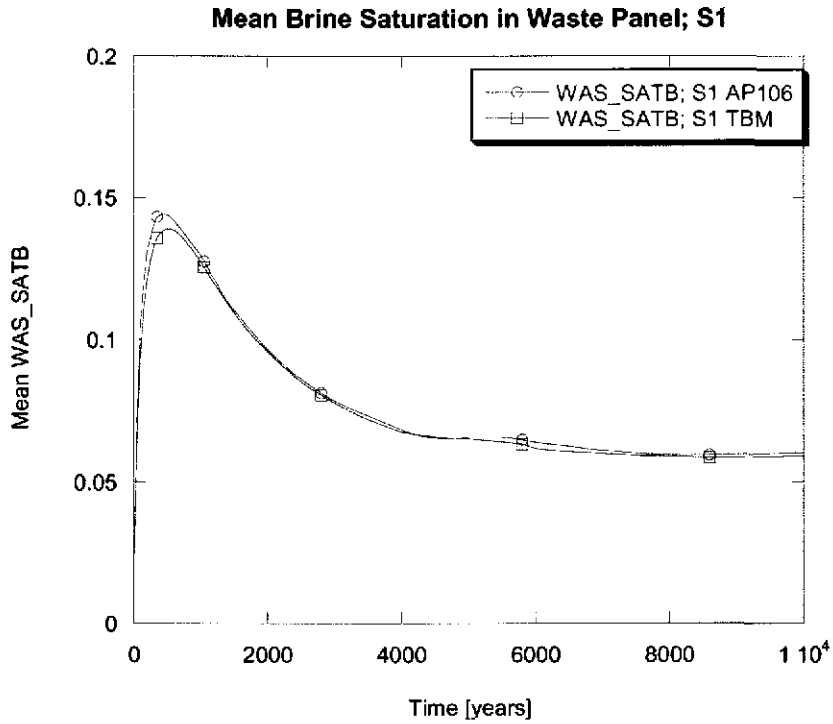

Figure 25. Average brine saturation in the waste panel for the AP106 and TBM S1 scenario.

Information Only

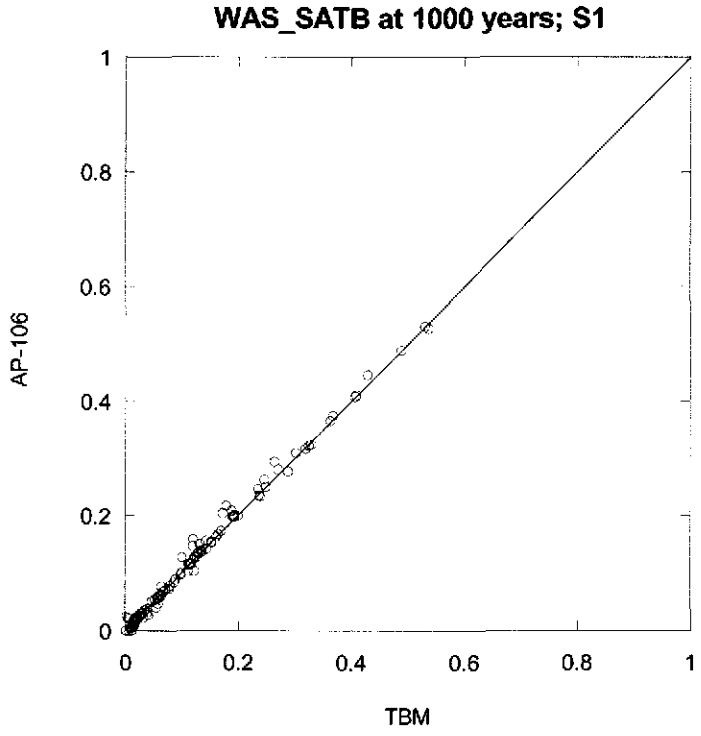

Figure 26. Scatter plot of brine saturation in the waste panel at 1,000 years; S1

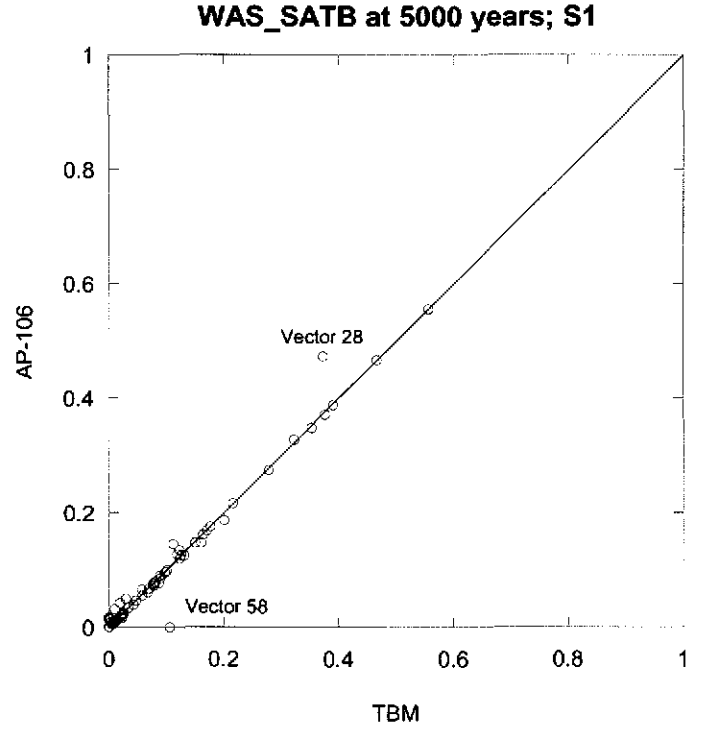

Figure 27. Scatter plot of brine saturation in the waste panel at 5,000 years; S1

Information Only

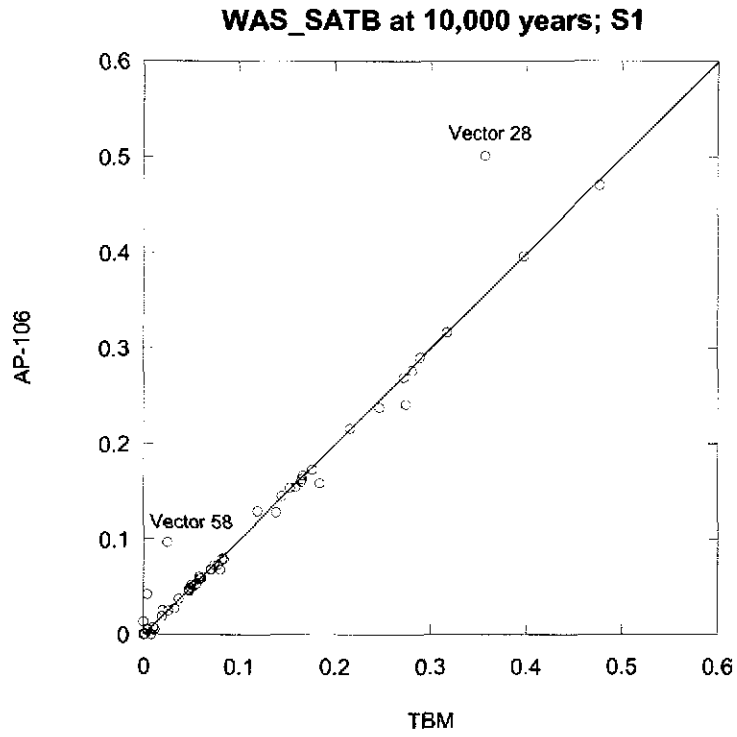

Figure 28. Scatter plot of brine saturation in the waste panel at 10,000 years; S1

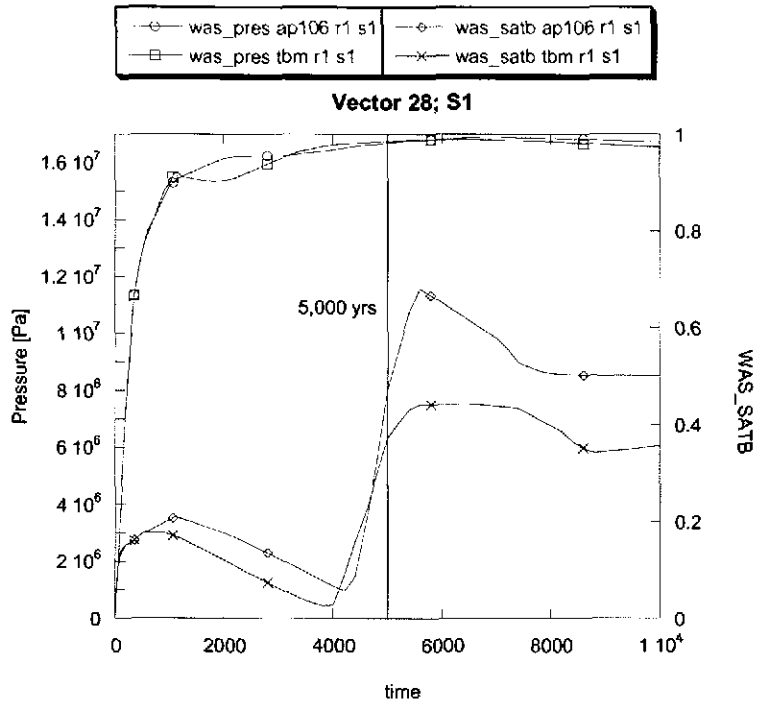

Figure 29. Detailed plot of pressure and brine saturation time histories for vector 28; S1

Information Only

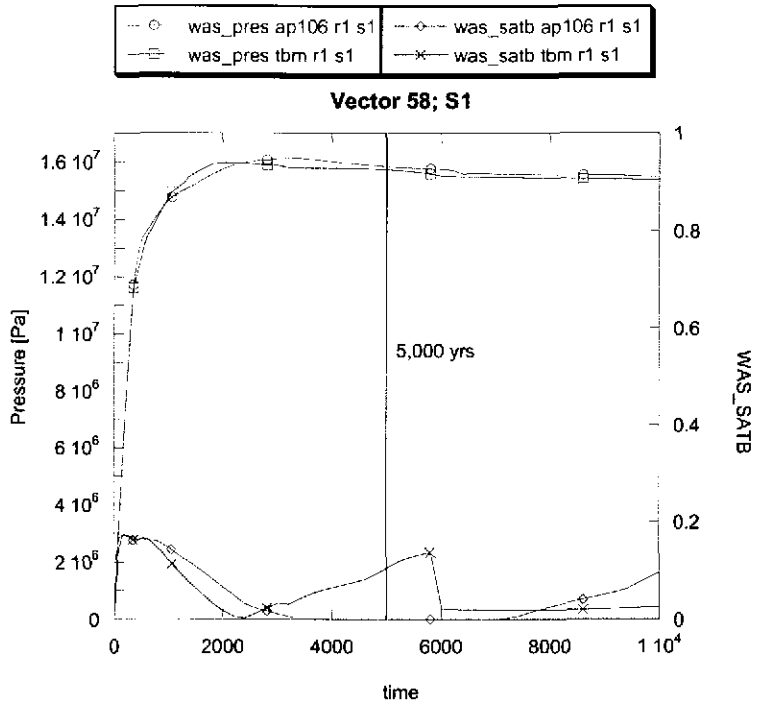

Figure 30. Detailed plot of pressure and brine saturation time histories for vector 58; S1

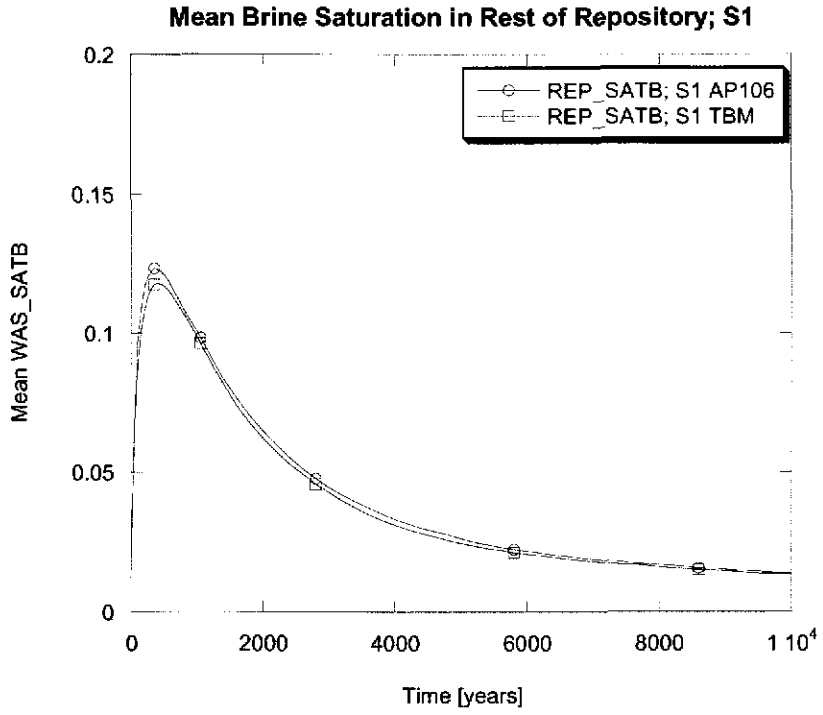

Figure 31. Average brine saturation in the rest of repository for the AP106 and TBM S1 scenario.

Information Only

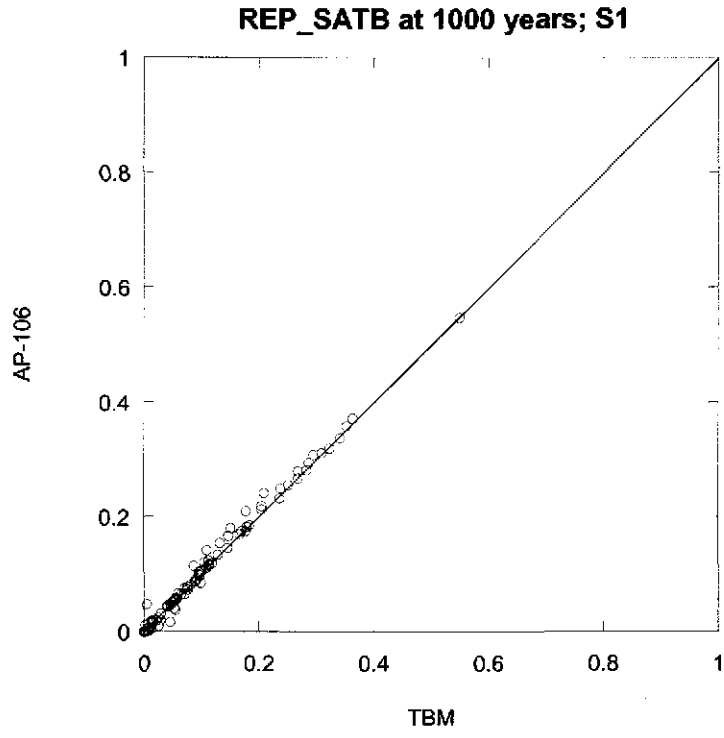

Figure 32. Scatter plot of brine saturation in the rest of repository at 1,000 years; S1

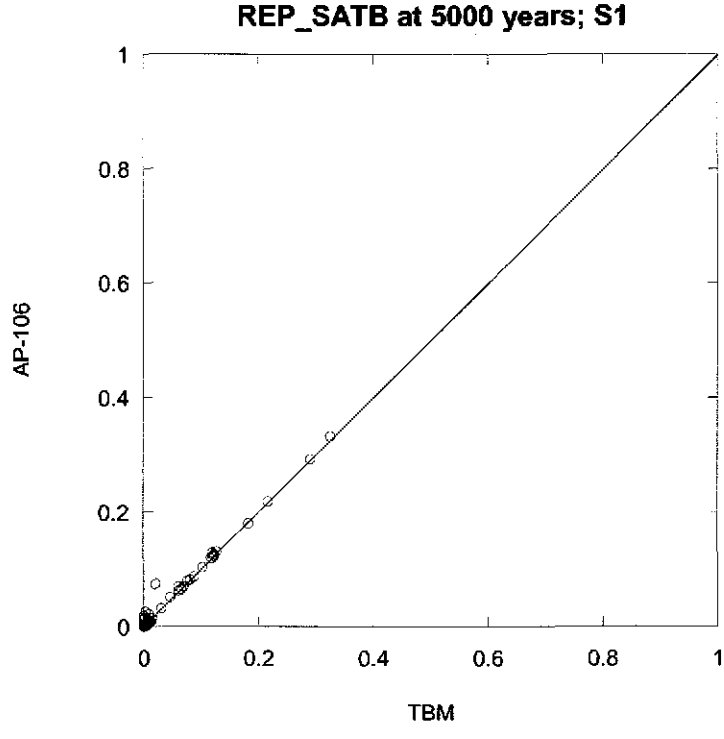

Figure 33. Scatter plot of brine saturation in the rest of repository at 5,000 years; S1

Information Only

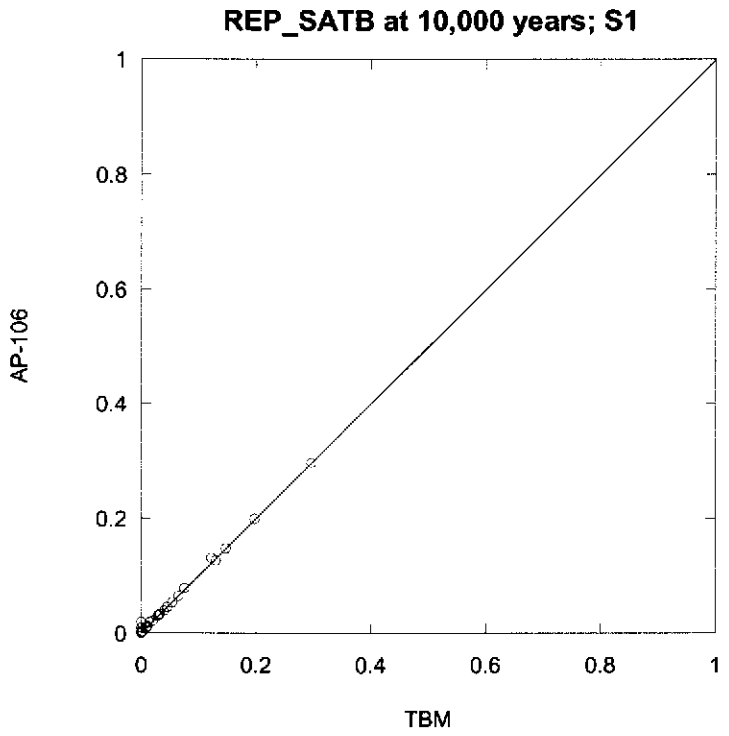

Figure 34. Scatter plot of brine saturation in the rest of repository at 10,000 years; S1

4.2.2 S3 Brine Saturations

Figure 35 shows the average brine saturation in the waste panel (WAS_SATB) for all 100 vectors in the S3 scenario for the AP106 and TBM calculations. Average brine saturation is somewhat higher in TBM than AP106. Figures 36 and 37 show scatter plots of WAS_SATB at 2,000 and 10,000 years. Vector-by-vector differences are minor for most vectors but a number of vectors show significant differences, with AP106 having lower saturations following the intrusion. We have chosen two vectors (vectors 10 and 27) to examine the cause of these differences. Figures 38 and 39 show detailed time histories of pressure and saturation for these vectors.

The S3 scenario models a brine pocket intrusion at 1,000 years. The consequences of this intrusion depend on the pressure in the waste panel and the pressure in the brine pocket, which is sampled. If the hydraulic head (pressure head + elevation head) in the waste panel is lower than the hydraulic head in the brine pocket, brine will flow from the pocket into the panel. If this gradient is reversed, brine can flow from the panel to the brine pocket. In some vectors the head gradient between the panel and the brine pocket is very small (pressures are nearly equal) and slight changes in pressures in the waste panel can have significant effects on brine flow in the borehole. Vectors 10 and 27 are two such vectors. In the TBM these vectors have modest brine flow up the borehole from the brine pocket. The slightly higher pressures in AP106 immediately preceding the intrusion (figures 38 and 39)

Information Only

reduce the head gradient enough to significantly decrease the brine flow up the borehole. To illustrate this we have plotted the sampled brine pocket pressure corrected for the elevation difference between the brine pocket and the repository.[a] The differences in saturation in these vectors persist for the entire simulation. Despite a number of other vectors that exhibit differences in saturations in figures 36 and 37, the mean difference (figure 35) is quite minor.

Figure 40 shows the average brine saturation in the rest of repository (REP_SATB) for all 100 vectors in the S3 scenario for the AP106 and TBM calculations. Average brine saturation is slightly higher in AP106 than TBM. Figures 41 and 42 show scatter plots of REP_SATB at 2,000 and 10,000 years. Vector-by-vector differences are minor in all cases.

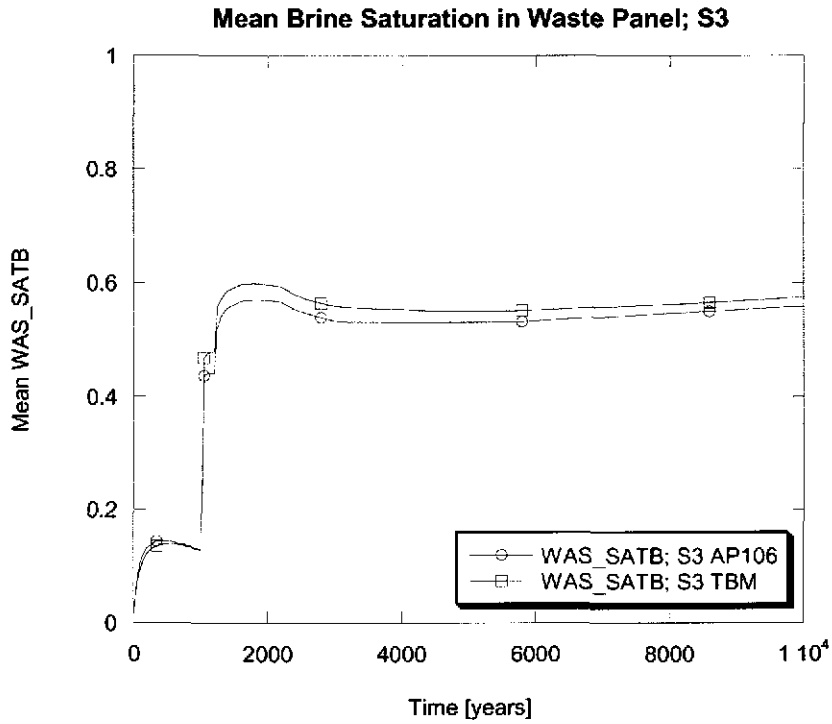

Figure 35. Average brine saturation in the waste panel for the AP106 and TBM S3 scenario.

a Elevation corrected brine pocket pressure equals sampled brine pocket pressure minus the product ρgh, where ρ is the brine density (1200 kg/m^3), g is gravitational acceleration used by BRAGFLO (9.79 m/s^2), and h is the vertical distance from the brine pocket to the repository (382 m).

Information Only

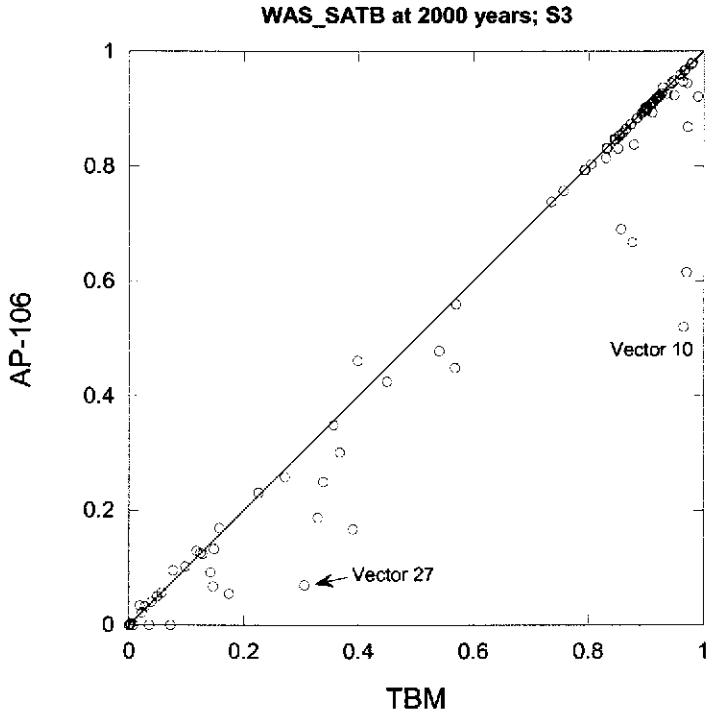

Figure 36. Scatter plot of brine saturation in the intruded panel at 2,000 years; S3

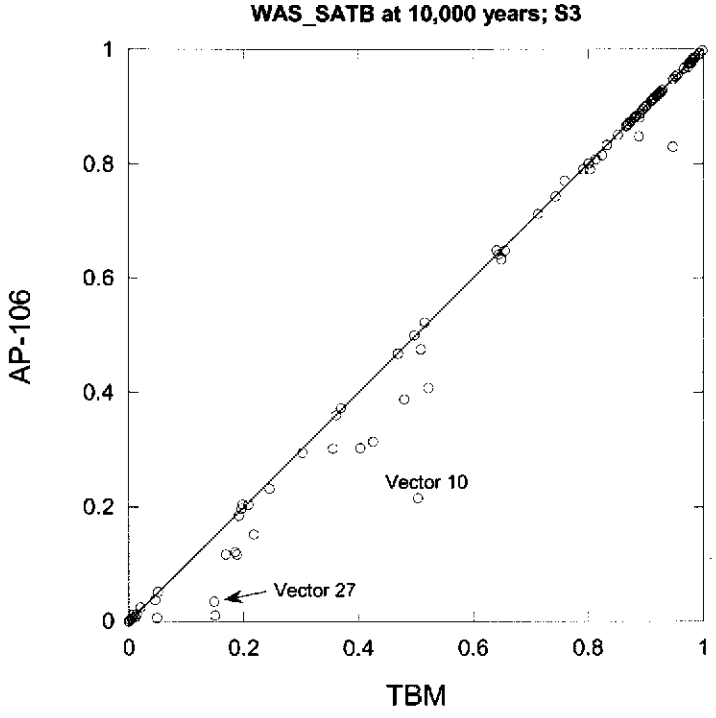

Figure 37. Scatter plot of brine saturation in the intruded panel at 10,000 years; S3

Information Only

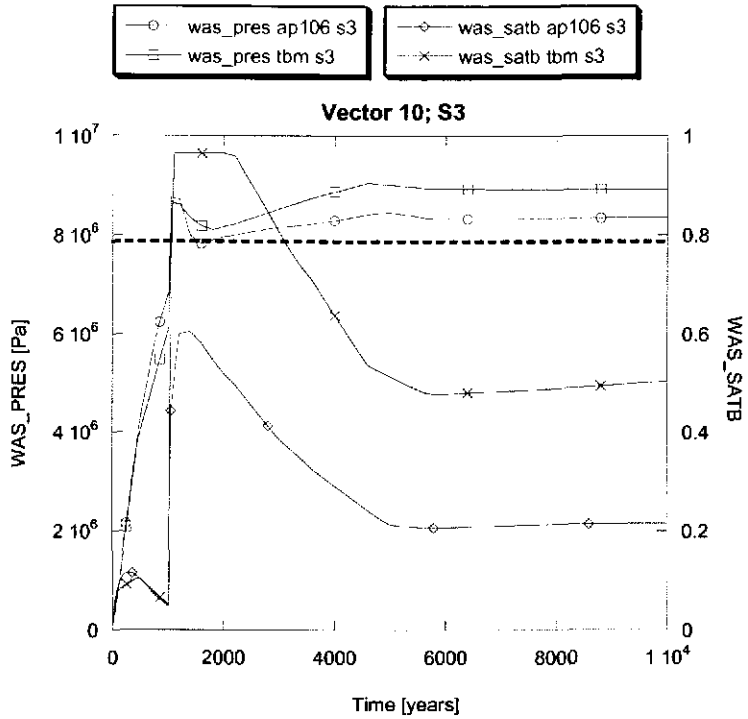

Figure 38. Detailed plot of pressure and brine saturation time histories for vector 10; S3. Dashed line is sampled brine pocket pressure at the elevation of the repository.

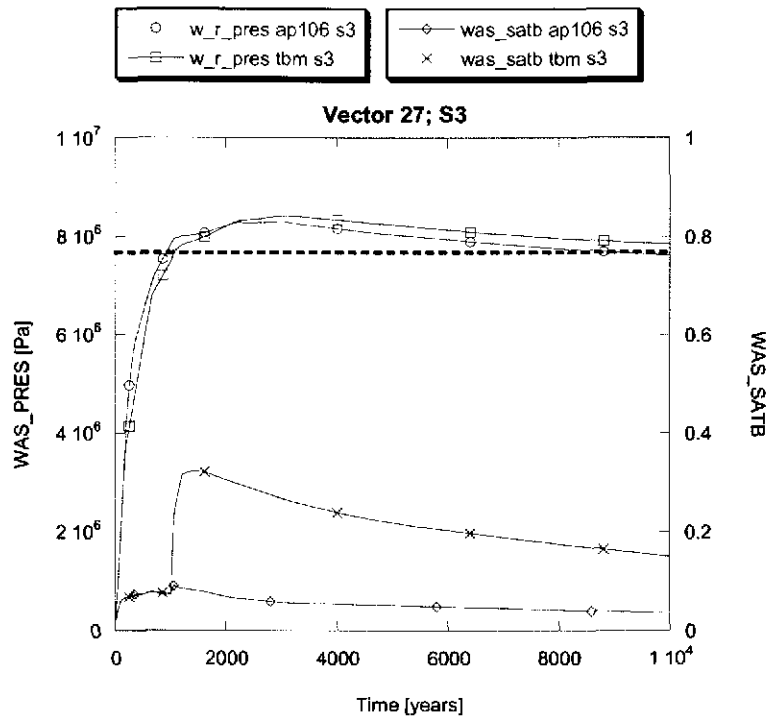

Figure 39. Detailed plot of pressure and brine saturation time histories for vector 27; S3. Dashed line is sampled brine pocket pressure at the elevation of the repository.

Information Only

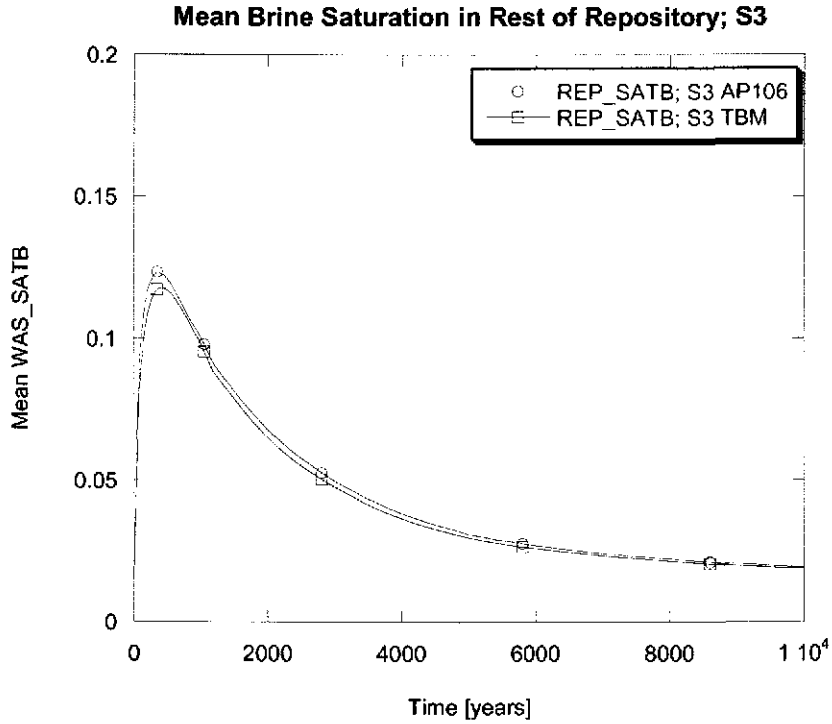

Figure 40. Average brine saturation in the rest of repository for the AP106 and TBM S3 scenario.

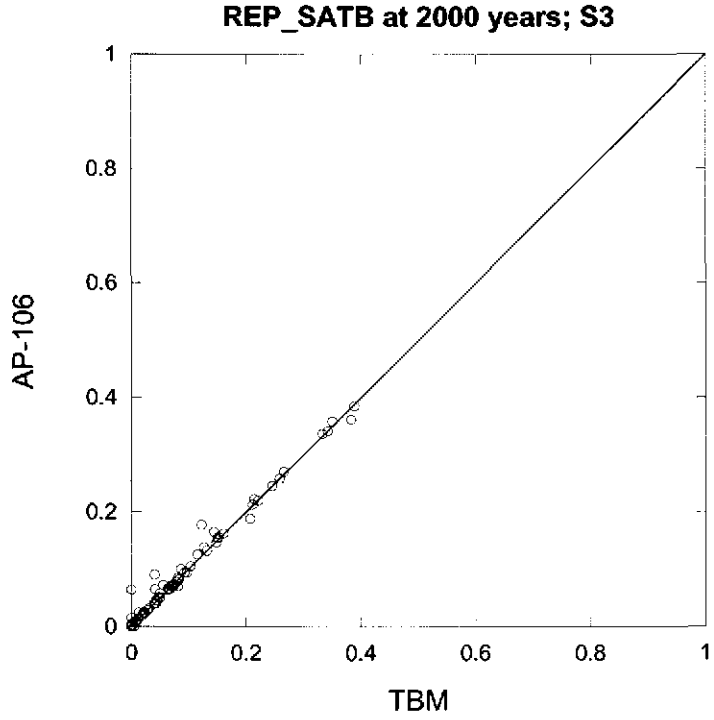

Figure 41. Scatter plot of brine saturation in the rest of repository at 2,000 years; S3

Information Only

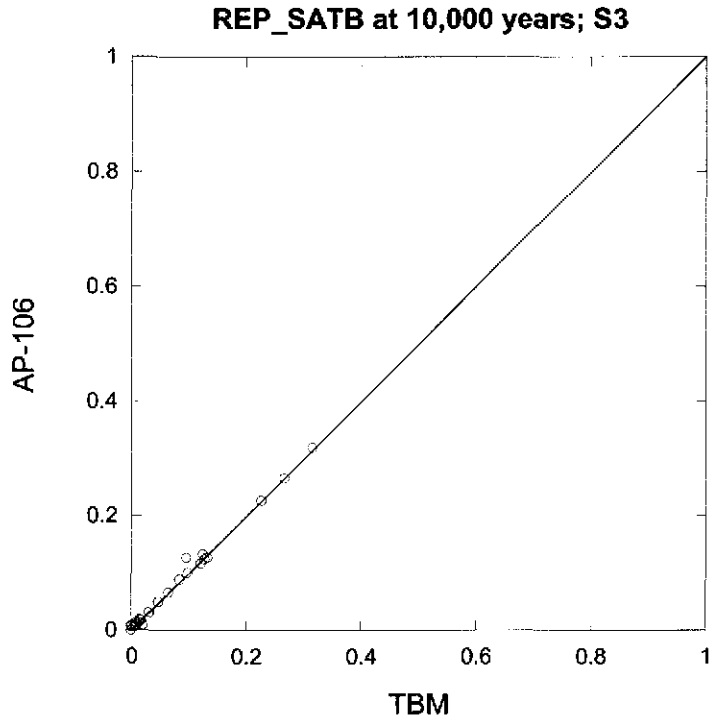

Figure 42. Scatter plot of brine saturation in the rest of repository at 10,000 years; S3

4.2.3 S5 Brine Saturations

Figure 43 shows the average brine saturation in the waste panel (WAS_SATB) for all 100 vectors in the S5 scenario for the AP106 and TBM calculations. Average brine saturation is nearly equal in the AP106 and TBM calculations. Figures 44 and 45 show scatter plots of WAS_SATB at 2,000 and 10,000 years. Vector-by-vector differences are minor for most vectors but a small number of vectors show significant differences, with AP106 having both lower and higher saturations at 2,000 years following the intrusion. We have chosen vectors 58 and 72 for a detailed examination into the cause of these differences. Figures 46 and 47 show detailed time histories of pressure and saturation for these vectors.

The S5 scenario models a repository intrusion at 1,000 years that does not intersect a brine pocket. Interpreting the pressure and saturation results from this scenario is more complicated than for the S3 brine pocket intrusion because the source of incoming brine is down the borehole from overlying formations. This downward brine flow has to compete with upward gas flow from the repository, resulting in variable, unsaturated conditions in the borehole. Because of the competition between the brine and gas phases and the very sensitive relationship between phase saturation and phase permeability, the flow of these phases tends to vary quite rapidly between runs, with one time step allowing brine to flow down and the next time step allowing gas to flow up. In order to plot pressure and saturation

Information Only

results from various calculations on a single plot we interpolate pressures and saturations to common times (typically every 100 years). Much of the dynamic behavior seen in pressure and saturation for the S5 scenario occurs over much shorter time periods and is therefore obscured in the process of interpolation.

Figure 46 shows an interpolated time history of pressures and saturations for vector 58. Vector 58 has lower saturations in AP106 than in TBM at 2,000 years but switches to higher saturations in AP106 than TBM by 10,000 years. This vector has high enough pressures that fracturing is occurring in the DRZ and the differences between calculations are due to the effects of implementing fracturing in the upper DRZ in the AP106 calculation.

Figure 47 shows an interpolated time history of pressures and saturations for vector 72. Pressures in this vector are below the fracturing threshold. AP106 pressures are higher than the TBM because of the double-wide panel closure (see section 3.1.1). After the intrusion, pressures and saturations are higher in AP106 than TBM until about 3,000 year when they match for the remainder of the run. An examination of the detailed time-step history of this vector indicates that very short-lived and highly variable flows of brine and gas occur in the borehole following the intrusion. This transient behavior results in the differences between interpolated pressure and saturation histories shown in figure 47. While these differences are interesting they do not warrant an exhaustive analysis, especially since figures 19 and 43 show that there is no significant, systematic difference in pressures or saturations between AP106 and TBM for this scenario.

Figure 48 shows the average brine saturation in the rest of repository (REP_SATB) for all 100 vectors in the S5 scenario for the AP106 and TBM calculations. Average brine saturation is nearly equal in the AP106 and TBM calculations. Figures 49 and 50 show scatter plots of REP_SATB at 2,000 and 10,000 years. Vector-by-vector differences are minor for all vectors.

Information Only

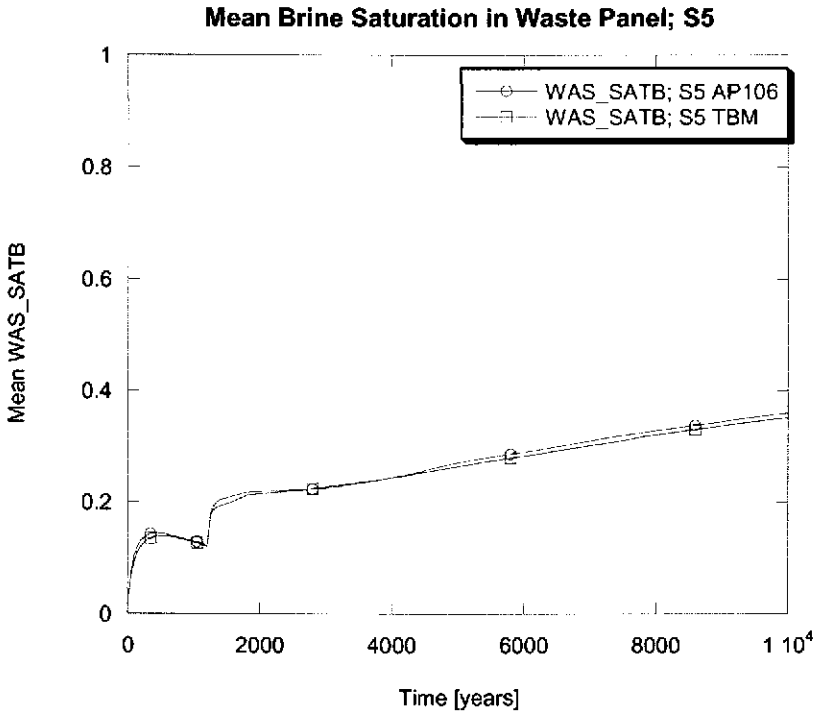

Figure 43. Average pressure in the waste panel for the AP106 and TBM S5 scenario.

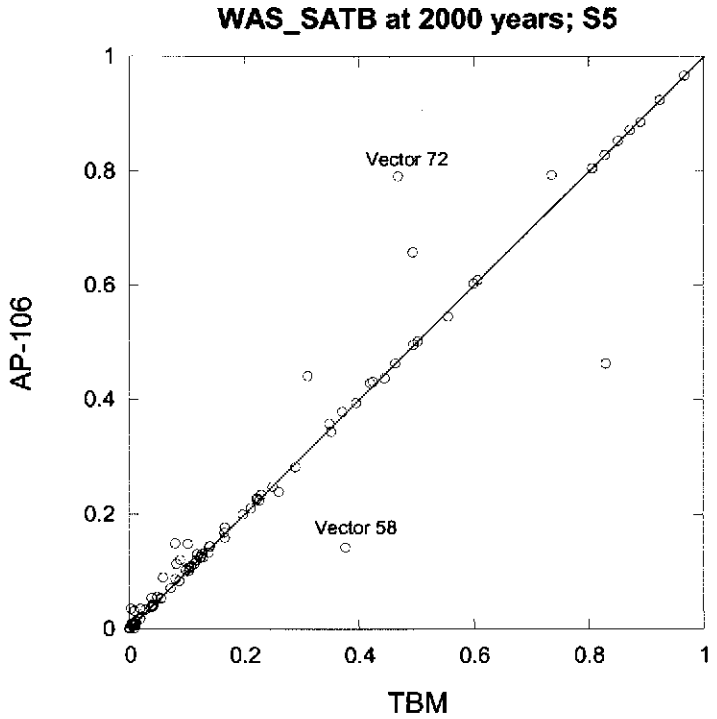

Figure 44. Scatter plot of brine saturation in the intruded panel at 2,000 years; S5

Information Only

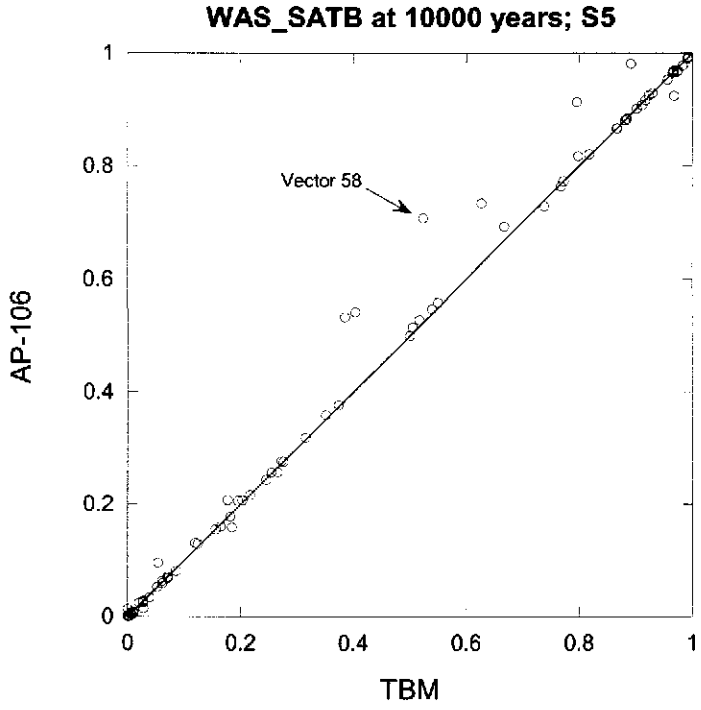

Figure 45. Scatter plot of brine saturation in the intruded panel at 10,000 years; S5

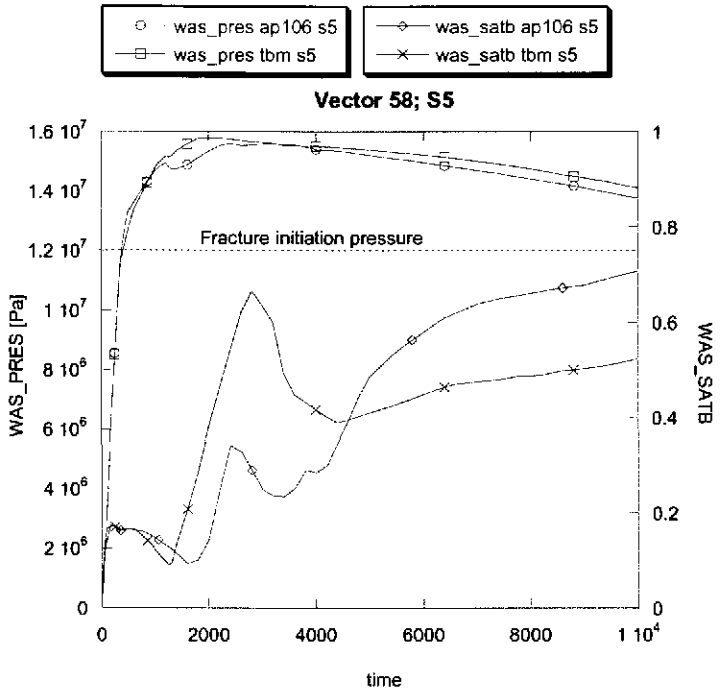

Figure 46. Detailed plot of pressure and brine saturation time histories for vector 58; S5

Information Only

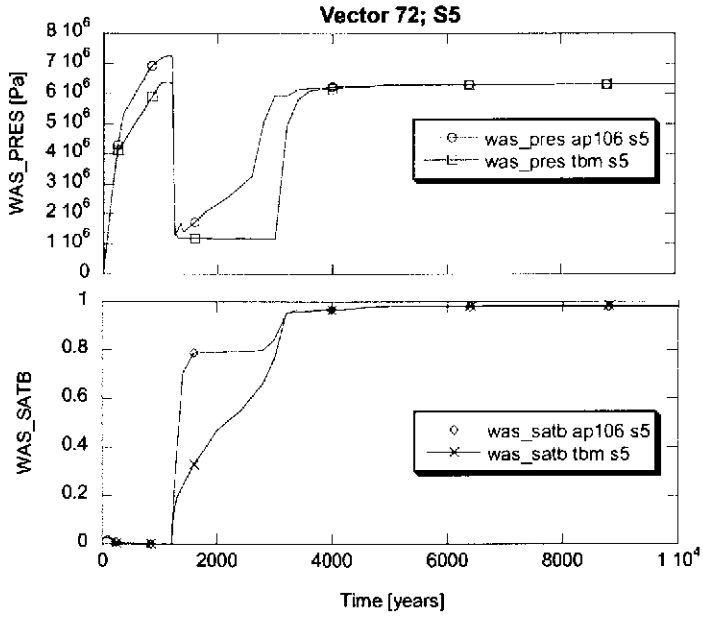

Figure 47. Detailed plot of pressure and brine saturation (separate plots for clarity) time histories for vector 72; S5

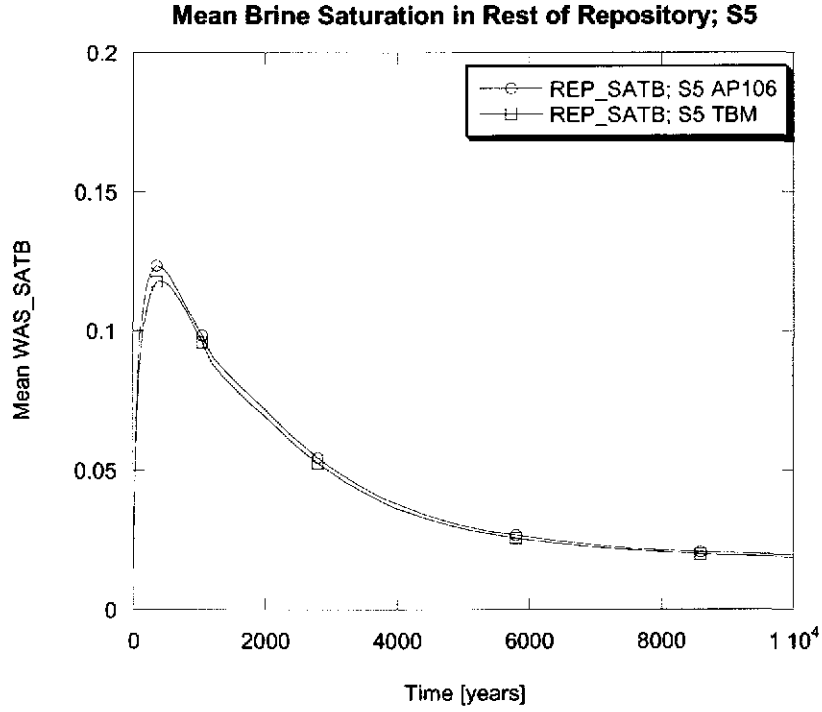

Figure 48. Average pressure in the rest of repository for the AP106 and TBM S5 scenario.

Information Only

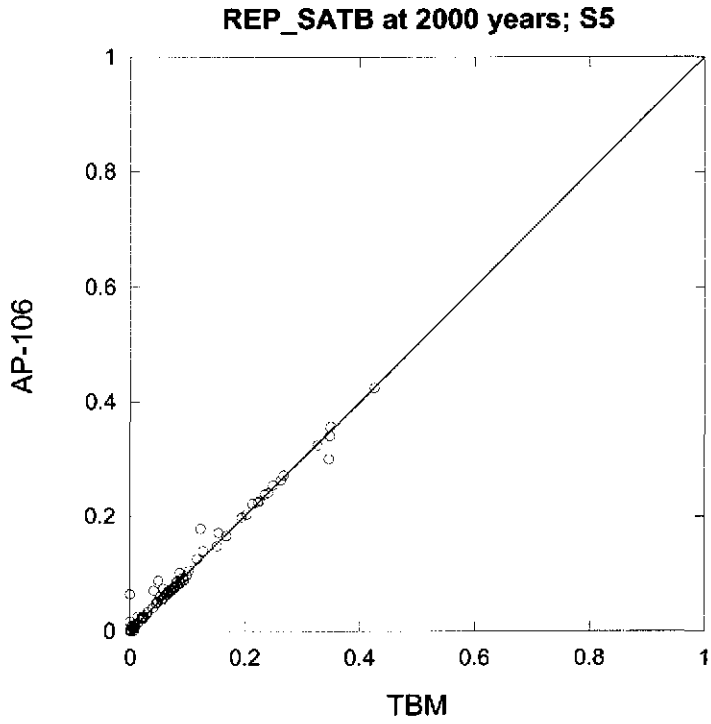

Figure 49. Scatter plot of brine saturation in the rest of repository at 2,000 years; S5

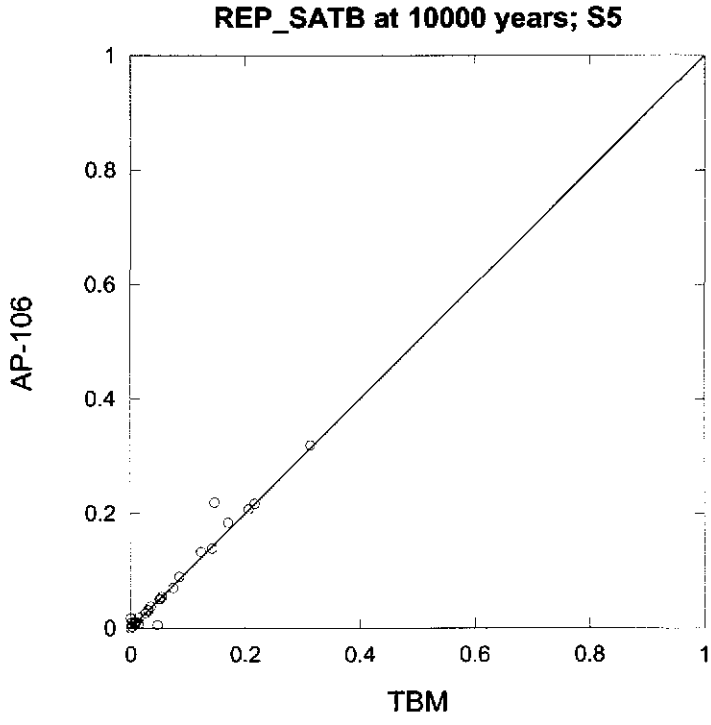

Figure 50. Scatter plot of brine saturation in the rest of repository at 10,000 years; S5

Information Only

4.3 Performance of the Simplified Shaft

Whether to include a shaft seal model in the BRAGFLO grid was debated as part of the TBM analysis (Hansen et al, 2002). The PAVT (and CCA) included a detailed shaft model that required numerous parameters and preprocessing calculations to be conducted. The TBM removed the shaft from the grid based on the lack of flow in this feature. The AP106 analyses include a simplified shaft seal model (James and Stein, 2003). To demonstrate that the simplified shaft seal model used in the AP106 calculations is a reasonable model we compare brine and gas flows in the simplified shaft model to flows in the PAVT detailed shaft seal model.

The simplified shaft seal model divides the shaft into upper and lower sections. The upper section is located above the Salado Formation, and is represented by the material, SHFTU. The lower section is located within the Salado Formation and is represented by the materials, SHFTL_T1 and SHFTL_T2 (SHFTL_T1 switches to SHFTL_T2 at 200 years). Where the lower section intersects Marker Bed 138 and Anhydrite AB, these cells are assigned to Marker Bed material.

The PAVT analysis incorporated 9 different materials for the shaft with six changes in properties at different times. Figure 51 compares the PAVT and simplified shaft model used in AP106.

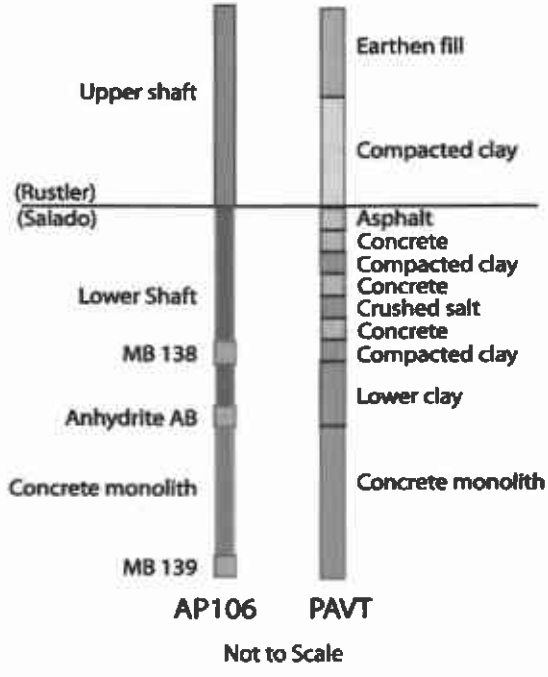

Figure 51. Comparison of the simplified shaft (AP106) and the detailed shaft (PAVT) models. Not to scale. Shown with logical dimensions.

In the present analysis, we compare average brine and gas flows at nine locations along the shaft to determine how flows differ between the simplified shaft

Information Only

model and the PAVT shaft model. Detailed flow data for the PAVT R1 was extracted using a revised post-ALGEBRA input file[b]. Table 2 presents the average cumulative flow of brine and gas for all 100 vectors at selected stratigraphic locations in the shaft.

Table 2: Comparison of modeling results of flow in the shaft from AP106 and the PAVT.

Flow Type	Stratigraphic Location	AP106 [m^3]	PAVT [m^3]
Brine Flow Up	SantaRosa	0	0
Brine Flow Up	DeweyLake	0	0
Brine Flow Up	Tamarisk	0.9	0.1
Brine Flow Up	Culebra	0.8	9.6
Brine Flow Up	Unnamed	2.1	9.8
Brine Flow Up	Salado	9.6	10.9
Brine Flow Up	MB138	7.9	10.4
Brine Flow Up	upperDRZ	0.2	0.4
Brine Flow Up	AnhydriteAB	0	0.4
Brine Flow Down	SantaRosa	0	9.3
Brine Flow Down	DeweyLake	183.2	198.0
Brine Flow Down	Tamarisk	244.2	97.1
Brine Flow Down	Culebra	27.1	31.6
Brine Flow Down	Unnamed	9.0	30.3
Brine Flow Down	Salado	5.1	10.4
Brine Flow Down	MB138	5.1	10.0
Brine Flow Down	upperDRZ	5.7	17.4
Brine Flow Down	AnhydriteAB	7.6	17.4
Gas Flow Up	SantaRosa	0.1	0
Gas Flow Up	DeweyLake	0	0
Gas Flow Up	Tamarisk	0	0.1
Gas Flow Up	Culebra	0	9.6
Gas Flow Up	Unnamed	0	9.8
Gas Flow Up	Salado	1379.1	10.9
Gas Flow Up	MB138	1093.8	10.4
Gas Flow Up	upperDRZ	16.0	0.4
Gas Flow Up	AnhydriteAB	196.0	0.4

[b] File is PAVT_BF_ALG2_AP106.INP and is located in LIB_AP106_P1_S0 and in LIBBF.

Information Only

Average brine flow up the shaft did not exceed 11 cubic meters for the entire 10,000 years at any point along the shaft in either analysis, and no brine flow rose above the middle Rustler in any vector. Average brine flow to the Culebra decreased from 9.6 m^3 in the PAVT to 0.8 m^3 in AP106. This reduction does not affect releases to the Culebra since the amount of brine that enters the Culebra from the borehole is orders of magnitude greater than any brine flow from the shaft seal. For comparison, the average amount of brine that entered the Culebra up the borehole in the AP106 S3 scenario is 5.29×10^4 m^3.

Brine flow down the shaft only occurred in the upper portion of the shaft, and this was entirely dependent upon the permeability of the upper shaft material in both AP106 and PAVT flow models. There is no potential impact on the repository, because only 5 cubic meters of the downward fluid flow reaches the concrete monolith in 10,000years.

In AP106, upward gas flow is seen in the Salado above the repository but is not seen in the PAVT model. This is probably due to the simplified shaft having a higher permeability in this region than the compacted salt material in the PAVT model. Even so, only minor gas flow occurred in AP106 in the lower Rustler, amounting to less than 10 cubic meters in 10,000 years, and no upwards gas flow penetrated above the Culebra in any vector.

To put these flows into perspective we can compare them to the total pore volume of the modeled shaft above the repository. The shaft volume is 62,130 m^3 (10 m x 654 m x 9.5 m). Using the porosity of the lower section (~0.11), an approximation of the total pore volume of the shaft is 6,834 m^3 (62,103 x 0.11). Compared to this value, the average flow of brine and gas in both shaft models is especially low.

In conclusion, flows of brine and gas from AP106 were very similar to results from the PAVT, and they support the conclusion that the shaft remains an unlikely pathway for any release, given our current conceptual models of the repository. Some results differ between the models but none of the differences contribute to potential releases. For example, gas flow within the upper Salado above the repository is significantly greater in AP106 than in the PAVT, however this difference is quite minor when compared with the total pore volume of the shaft. In addition, brine flow up the shaft to the Culebra decreased in AP106 but will not affect Culebra releases because (1) the amount of brine entering the Culebra from the borehole far exceeds any brine contributions from the shaft and (2) such small volumes of brine are unlikely to have ever contacted waste which is hundreds of meters below the Culebra. Even with these minor differences, the simplified shaft model functions very much like the more detailed shaft model in that it remains an effective barrier to releases.

4.4 Spallings CCDF Results

During the Salado Peer Review meetings in February, 2003 the panel requested an analysis of how the AP106 BRAGFLO results would affect WIPP PA

Information Only

results, namely the CCDF results used to measure performance. We showed the panel the CCDF results of the TBM (Dunagan, 2003), and they were interested to hear how the modifications made to the TBM for this analysis might affect CCDF results. To make this assessment, we dealt with each release mechanism that contributes to the total release CCDF separately.

The largest contributor to the total releases CCDF is the combined releases from cuttings and cavings. Since these releases do not depend on any variables from BRAGFLO, this release would be identical for the AP106.

The second largest contributor to the total releases CCDF is the spallings release. Spallings releases are solid releases entrained by gases flowing up and out a borehole immediately following an intrusion. The cuttings, cavings, and spallings releases combined account for more than 99% of the total releases and therefore will provide a very accurate estimate of the total releases assuming AP106 BRAGFLO results. The other releases (direct brine releases, Culebra, and Salado releases) are at least two orders of magnitude below the combined cuttings, cavings, and spallings releases. The BRAGFLO results could increase these other releases but only if pressures and saturations increases well above present levels. Given current conceptual models, there is no reasonable way for these minor releases to increase enough to become more important than cuttings, cavings, or spallings.

Spallings releases were calculated using the model approved for the PAVT. In this model, any time an intrusion occurs a spallings release occurs as long as pressures in the intruded panel exceed 8 MPa at the time of intrusion. The volume of each spallings release is randomly sampled between 0.5 and 4 m^3. The concentration of radionuclides in the spallings release is calculated assuming the waste is homogeneously mixed and distributed throughout the repository. Currently, progress is being made on implementing a new mechanistic model for spallings, but this model must first pass peer review before it can be used for compliance calculations and therefore was not used in the present analysis.

To calculate the spallings CCDF we ran two additional BRAGFLO scenarios (S2 and S4) that are required by CCDFGF. We then ran CUTTINGS_S using the AP106 BRAGFLO results as input, followed by CCDFGF, using the AP106 CUTTINGS_S files as inputs, and using TBM files for the remaining inputs to CCDFGF. CCDFGF cannot be fine tuned to calculate just one component CCDF so we needed to calculate all the CCDFs and then only retain the spallings CCDF that only depends on BRAGFLO results.

Figure 52 shows the mean spallings CCDF from AP106 and from the TBM calculations (Dunagan, 2003). The curves are so similar it is hard to see any differences. The regulations are based on the mean CCDF so it is clear that the changes made for the AP106 runs have virtually no effect on mean spallings releases. Figure 53 shows the median, 90^{th}, and 10^{th} percentile CCDFs. It is evident in this figure that the AP106 has a slightly higher median but this difference is not significant.

Information Only

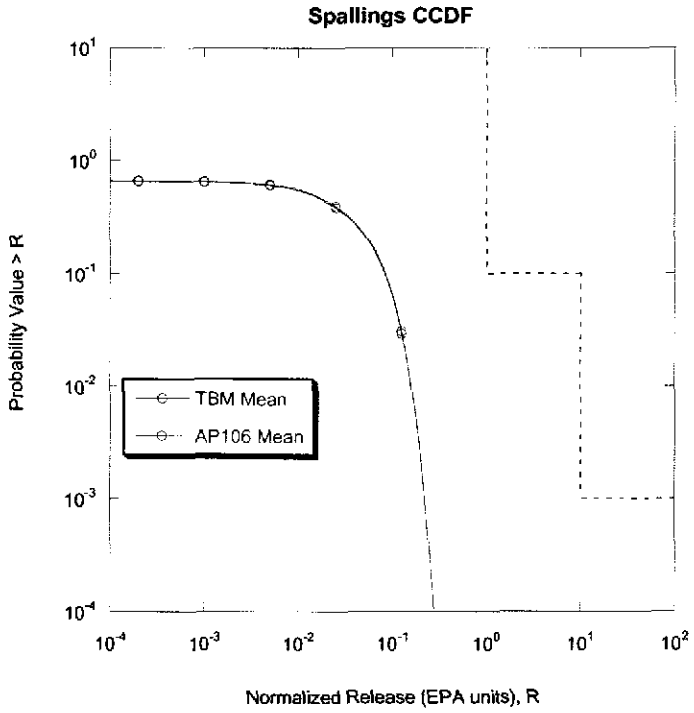

Figure 52. Mean spallings CCDF results from AP106 and TBM.

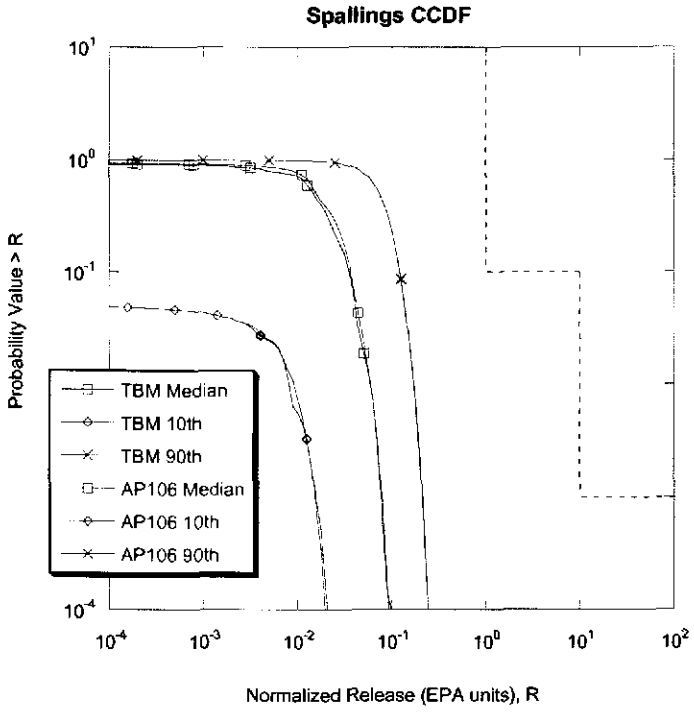

Figure 53. Median, 90th, and 10th spallings CCDF results from AP106 and TBM.

Information Only

5 JUSTIFICATION OF CLAY SEAM "G"MODELING ASSUMPTIONS

As part of the effort to determine if the change in repository horizon warrants more detailed consideration in the model grid, we ran an additional undisturbed scenario (S1) in which we adjusted the porosity of the upper and lower DRZ to simulate the thinning of the upper DRZ and thickening of the lower DRZ in the half of the repository that will be raised to Clay Seam "G".

One effect of moving the southern half of the repository up to Clay Seam G is that the floor of this half of the repository will ramp up ~2.4 meters. In the original BRAGFLO grid used for the CCA and PAVT the repository was at a single stratigraphic level, but it dipped to the south by 1 degree. From a permeability standpoint, fluids were relatively free to communicate between panels and across permeable panel closures. As a result, brine tended to flow down dip and collected in the single waste panel represented at the south end of the repository in the model grid. This resulted in higher brine saturations in this panel than in the rest of the repository. As part of the changes incorporated for the TBM, Option D panel closures were added into the grid and had the result that fluids no longer were able to easily flow between panels due to the impermeable panel closures. The TBM conceptual model results in the repository being more segmented than in the open CCA/PAVT conceptual model and the undisturbed brine saturations in all the waste regions are essentially equivalent. Because the Option D panel closures are so effective in preventing brine from flowing between panels, adding a ramp up to the southern half of the repository will not affect brine flow patterns due to the 1-degree dip. For this reason SNL advises that the horizon change need not be included explicitly in the model grid.

Another effect of the horizon change is to change the thickness of the upper and lower DRZ. This was discussed in section 2.2 in relation to the justification for including fracturing in both the upper and lower DRZ. The thickness of the DRZ is important not only in relation to flow pathways, but also in relation to total pore volume in the DRZ, and brine availability to the waste. A significant portion of the brine that contacts the waste and allows gas generation reactions to proceed comes from the DRZ in the first couple of hundred of years (Hansen et al., 2002). In the raised repository, the upper DRZ will be 2.4 meters thinner and the lower DRZ will be thicker by 2.4 meters.

6 RESULTS PART 2

We defined an "excursion" set of 100 vectors from the undisturbed scenario, which we will hereafter refer to as the S1_P2 scenario. In these S1_P2, runs the porosity of the upper and lower DRZ in the southern half of the repository was adjusted to account for the *effect* of changing the DRZ thickness without actually changing the thickness. Specifically, we reduced the porosity in the upper DRZ directly over the southern half of the waste areas (single waste panel and southern rest of repository blocks) so that the total pore volume in these grid cells is equal to the

Information Only

total pore volume expected in the thinner DRZ. A similar practice was used in the lower DRZ, except that the porosity was increased proportionally to the increase in thickness of this layer. To evaluate how this change affects gas generation, pressure and brine saturation we compare results of the "excursion" runs with the AP106 results that were described in section 4.

6.1 S1_P2 Pressures

Figure 54 shows average pressure in the waste panel (WAS_PRES) for all 100 vectors in the S1 scenario for the AP106 and the S1_P2 calculations. Average pressures tend to be slightly higher in AP106 than S1_P2. Figures 55 and 56 show scatter plots of WAS_PRES at 1,000 and 5,000 years. Vector-by-vector differences are minor in all cases.

Figure 57 shows average pressure in the rest of repository (REP_PRES) for all 100 vectors in the S1 scenario for the AP106 and the S1_P2 calculations. Average pressures tend to be slightly higher in AP106 than S1_P2. Figures 58 and 59 show scatter plots of REP_PRES at 1,000 and 5,000 years. Vector-by-vector differences are minor in all cases.

Pressures are slightly lower in the S1_P2 runs because less brine enters the waste regions due to the reduced pore volume in the upper DRZ.

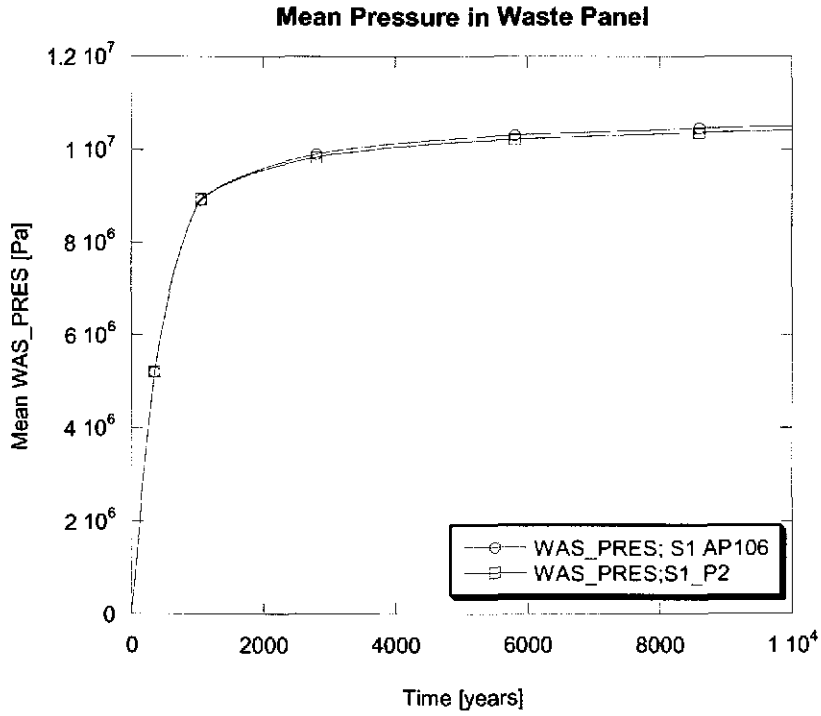

Figure 54. Average pressure in the waste panel for the AP106 S1 and S1_P2 runs.

Information Only

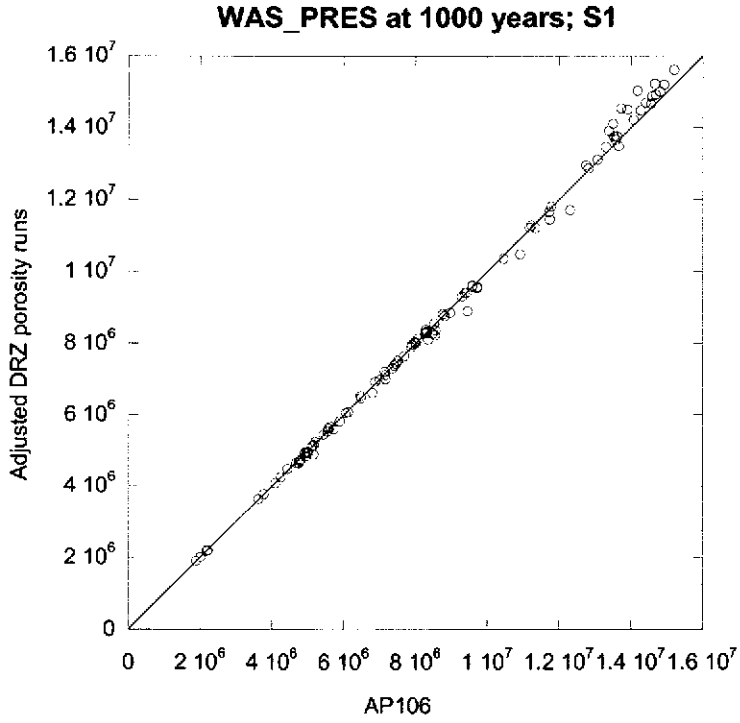

Figure 55. Scatter plot of pressure in the waste panel at 1,000 years; AP106 S1 vs. S1_P2

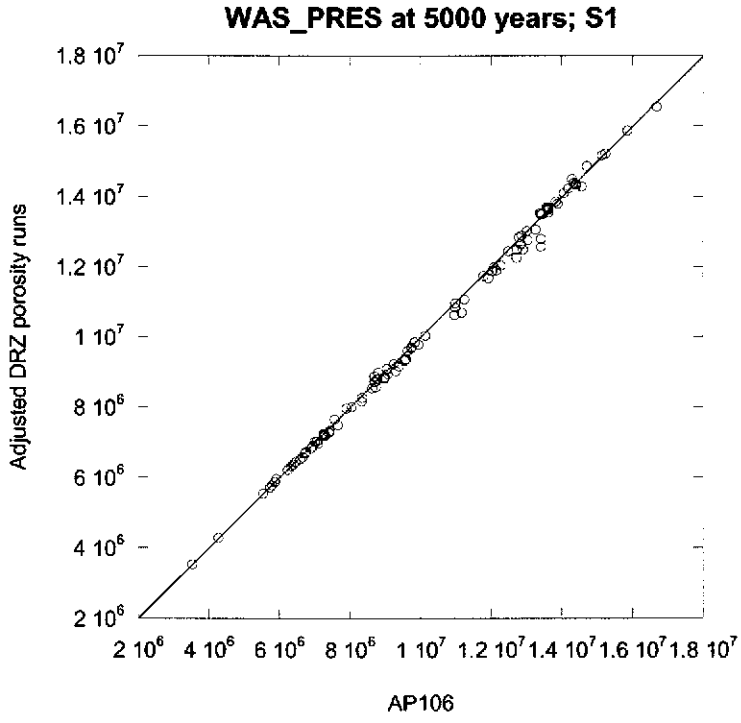

Figure 56. Scatter plot of pressure in the waste panel at 5,000 years; AP106 S1 vs. S1_P2

Information Only

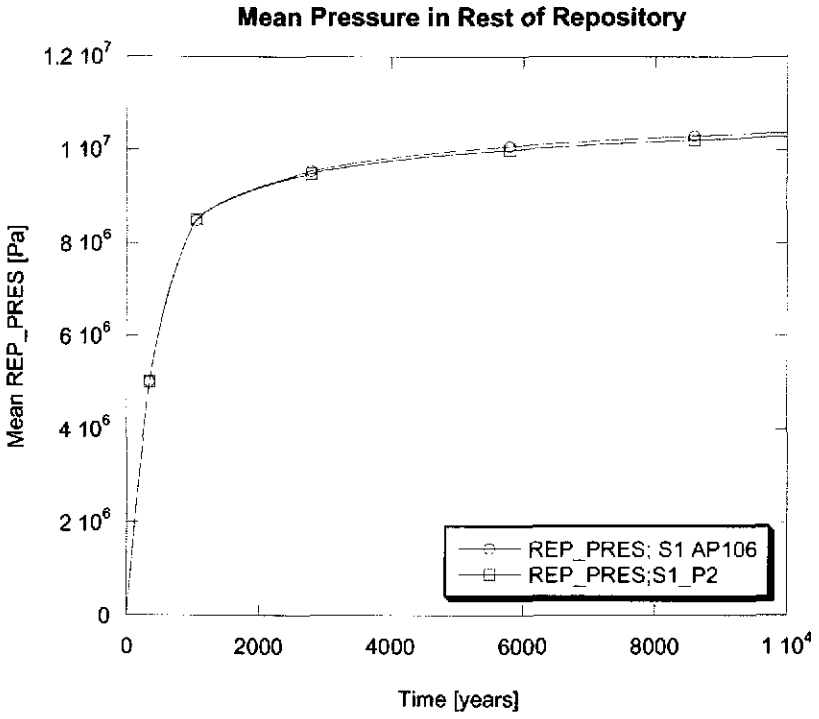

Figure 57. Average pressure in the rest of repository for the AP106 S1 and S1_P2 runs.

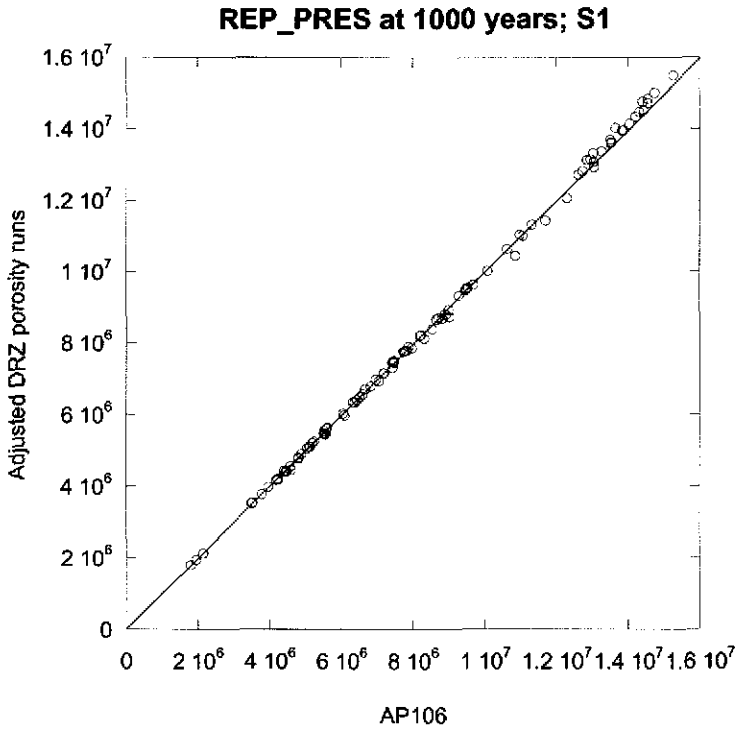

Figure 58. Scatter plot of pressure in the rest of repository at 1,000 years; AP106 S1 vs. S1_P2

Information Only

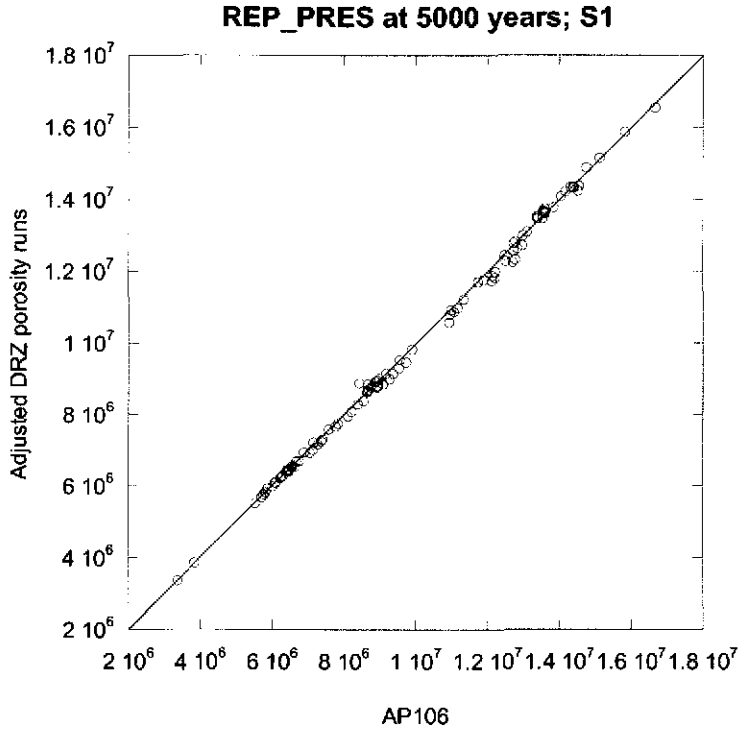

Figure 59. Scatter plot of pressure in the rest of repository at 5,000 years; AP106 S1 vs. S1_P2

6.2 S1_P2 Brine Saturations

Figure 60 shows average brine saturation in the waste panel (WAS_SATB) for all 100 vectors in the S1 scenario for the AP106 and the S1_P2 calculations. Average saturation is somewhat higher in AP106 than S1_P2, however the reduced scale on the saturation axis exaggerates this difference. Figures 61 and 62 show scatter plots of WAS_SATB at 1,000 and 5,000 years. Vector-by-vector differences show that saturation differences are systematic.

Vector 28 is the single outlier in figure 62. Figure 63 shows the detailed time history for this vector. This vector is the highest-pressure vector in both calculations and fracturing is well developed in the DRZ. Slight changes in pressure have significant effects on fracture permeability and variable saturation in the DRZ affects the relative permeability for each phase. In the S1_P2 simulation there is less available pore volume in the upper DRZ for storing excess gas and therefore pressures in this simulation are higher. These higher pressures in combination with less upper DRZ pore volume prevent any additional brine from entering the waste regions, resulting in near zero brine saturations by about 4,500 years.

Figure 64 shows average brine saturation in the rest of repository (REP_PRES) for all 100 vectors in the S1 scenario for the AP106 and the S1_P2 calculations. Average saturation tends to be higher in AP106 than S1_P2, but not to the extent seen in the waste panel (Figure 60). This is reasonable since the pore

Information Only

volume reduction only affects four of the nine panels represented in the full rest of repository. Figures 65 and 66 show scatter plots of REP_SATB at 1,000 and 5,000 years. Vector-by-vector differences are minor in all cases.

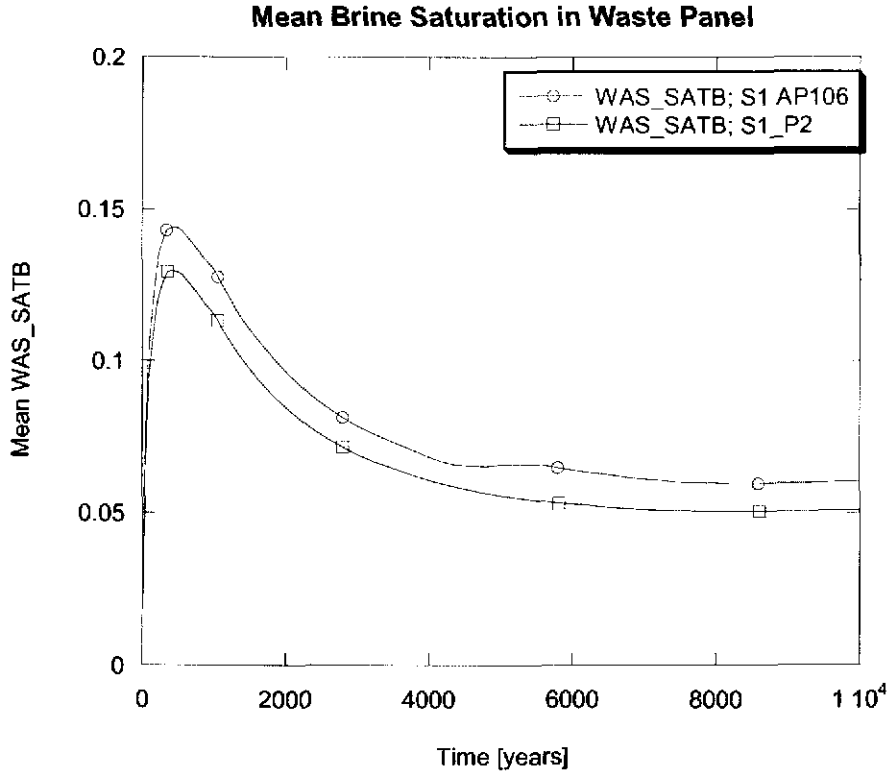

Figure 60. Average brine saturation in waste panel for the AP106 S1 and S1_P2 runs.

Information Only

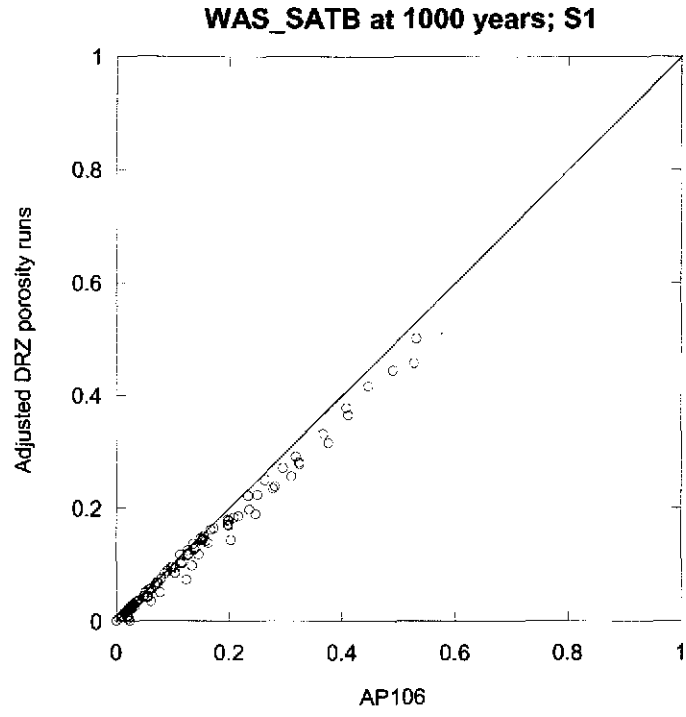

Figure 61. Scatter plot of brine saturation in the waste panel at 1,000 years; AP106 S1 vs. S1_P2

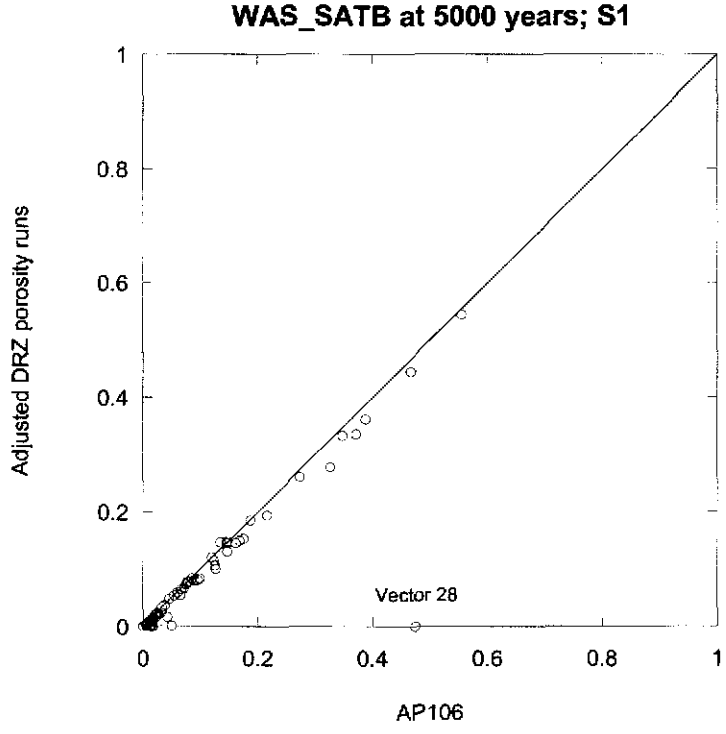

Figure 62. Scatter plot of brine saturation in the waste panel at 5,000 years; AP106 S1 vs. S1_P2

Information Only

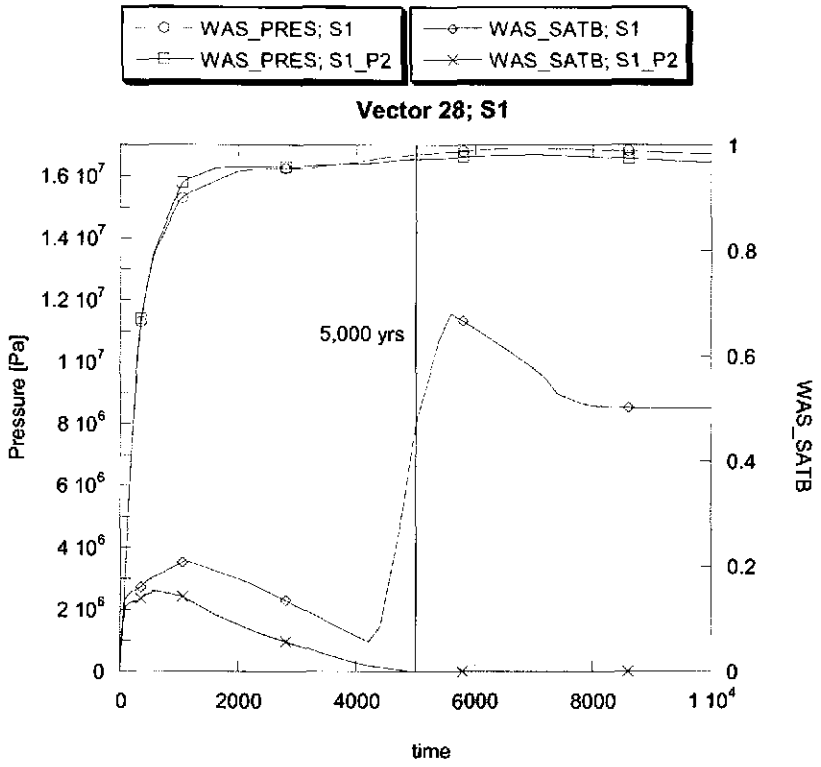

Figure 63. Detailed plot of pressure and brine saturation time histories for vector 28; AP106 S1 & S1_P2.

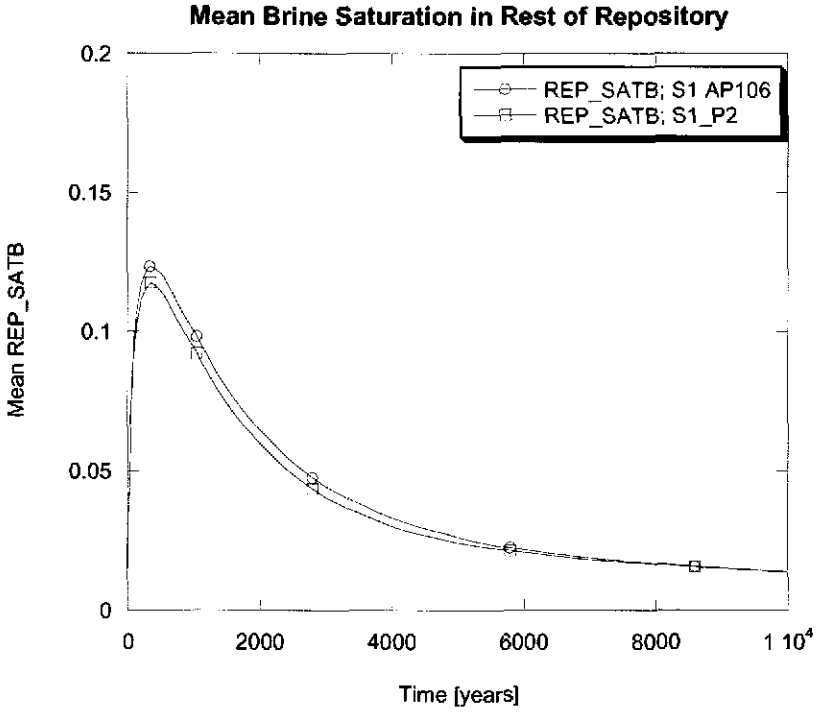

Figure 64. Average brine saturation in the rest of repository for the AP106 S1 and S1_P2 runs.

Information Only

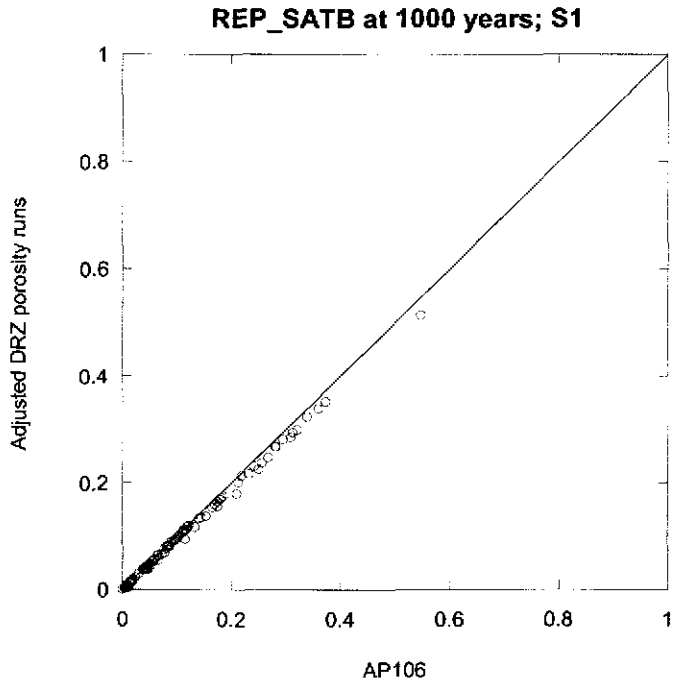

Figure 65. Scatter plot of brine saturation in the rest of repository at 1,000 years; AP106 S1 vs. S1_P2

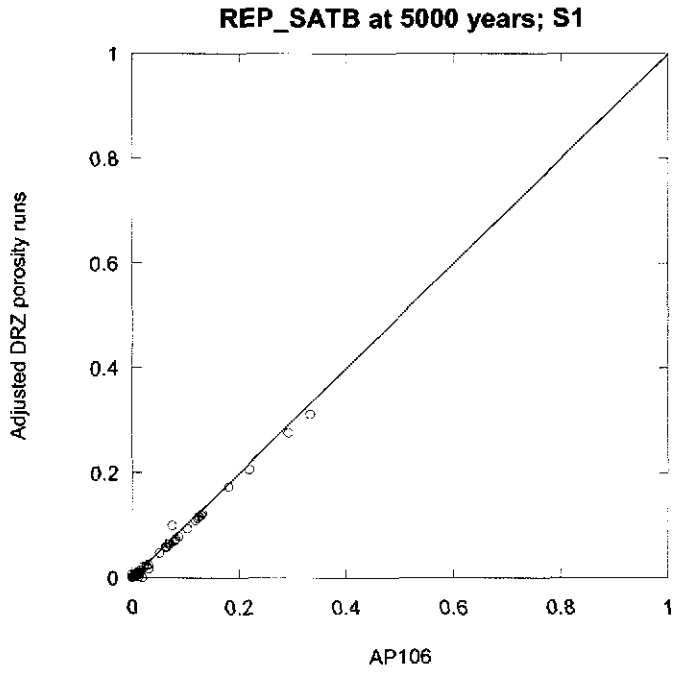

Figure 66. Scatter plot of brine saturation in the rest of repository at 5,000 years; AP106 S1 vs. S1_P2

Information Only

6.3 Conclusions

The changes made to the pore volume of the DRZ in the half of the repository that will be raised to Clay Seam "G" have no significant effect on BRAGFLO results of pressure and saturation. Generally, the effect of this change is to lower saturations in the raised half of the repository due to the reduced pore volume in the upper DRZ above this region. Only one vector, that has considerable fracturing, was significantly affected by the changes to the DRZ.

These results indicate that explicit representation of the Clay Seam "G" horizon change in the BRAGFLO grid is not warranted. In fact, by not including the horizon change explicitly, our results suggest that we will overestimate the brine saturation in the raised waste regions. This is a conservative assumption because higher saturations can lead to greater direct brine releases and Culebra releases.

7 CMS AND SOFTWARE INFORMATION

The codes that were used for these calculations are listed in Table 3. Calculations were performed on the ES-40 DEC ALPHA running Open VMS Version 7.3-1. All input and output files are stored in CMS libraries as documented in a separate memorandum (Coman, 2003).

Table 3. Codes used in this analysis.

Code	Version
ALGEBRACDB	2.35
BLOTCDB	1.37
BRAGFLO	4.10.02
CCDFGF	3.01
CUTTINGS_S	5.04A
GENMESH	6.08
ICSET	2.22
LHS	2.41
MATSET	9.10
POSTBRAG	4.00
POSTLHS	4.07
PREBRAG	6.00
PRELHS	2.10
SPLAT	1.02
SUMMARIZE	2.20

Information Only

8 REFERENCES

Caporuscio, F., Gibbons, J., and Oswald, E. 2002. *Waste Isolation Pilot Plant: Salado Flow Conceptual Models Peer Review Report*. Report prepared for the U.S. Department of Energy, Carlsbad Area Office, Office of Regulatory Compliance. ERMS# 523783.

Coman, R. 2003. "AP106 Run Control Documentation." Memorandum to Cliff Hansen dated March 19, 2003. ERMS# 526632.

DOE. 2000. "Letter from Dr. Triay to Mr. Marcinowski dated June 26, 2000."

Dunagan, S. 2003. "Complementary Cumulative Distribution Functions (CCDF) for the Technical Baseline Migration (TBM) Rev 0." Carlsbad, NM: Sandia National Laboratories. ERMS# 525707.

EPA. 2000. "Letter from Mr. Marcinowski to Dr. Triay dated August 11, 2000."

EPA. 2002a. "Letter from Mr. Marcinowski to Dr. Triay dated August 6, 2002."

EPA. 2002b. "Letter from Mr. Marcinowski to Dr. Triay dated December 13, 2002."

Hansen, C., Leigh, C., Lord, D., and Stein, J. 2002. "BRAGFLO Results for the Technical Baseline Migration." Carlsbad, NM: Sandia National Laboratories. ERMS# 523209.

Helton, J.C., Bean, J.E., Berglund, J.W., Davis, F.J., Garner, J.W., Johnson, J.D., MacKinnon, R.J., Miller, J., O'Brien, D.G., Ramsey, J.L., Schreiber, J.D., Shinta, A., Smith, L.N., Stoelzel, D.M., Stockman, C., and Vaughn, P. 1998. *Uncertainty and Sensitivity Analysis Results Obtained in the 1996 Performance Assessment for the Waste Isolation Pilot Plant*. SAND98-0365. Albuquerque, NM: Sandia National Laboratories.

James, S.J., and Stein, J. 2002. "Analysis Plan for the Development of a Simplified Shaft Seal Model for the WIPP Performance Assessment." AP-094. Carlsbad, NM: Sandia National Laboratories. ERMS# 524958.

James, S.J., and Stein, J. 2003. "Analysis Report for the Development of a Simplified Shaft Seal Model for the WIPP Performance Assessment Rev. 1." Carlsbad, NM: Sandia National Laboratories. ERMS# 525203.

Information Only

Park, B.Y. 2002. "Analysis Plan for Structural Evaluation of WIPP Disposal Room Raised to Clay Seam G." AP-093. Carlsbad, NM: Sandia National Laboratories.

SNL. 1996. *Waste Isolation Pilot Plant Shaft Sealing System compliance submittal design report.* SAND96-1326. Albuquerque, NM: Sandia National Laboratories.

Stein, J. 2002. "Minor difference found in TBM grid volumes." Memorandum to M.K. Knowles, May 20, 2002. Carlsbad, NM: Sandia National Laboratories. ERMS# 522357.

Stein, J., and Zelinski, W. 2003. "Analysis Plan for the Testing of a Proposed BRAGFLO Grid to be used for the Compliance Recertification Application Performance Assessment Calculations." AP-106. Carlsbad, NM: Sandia National Laboratories. ERMS# 525236.

Wawersik, W.R., and Stone, C.M. 1989. "A Characterization of Pressure Records in Inelastic Rock Demonstrated by Hydraulic Fracturing Measurments in Salt," *International Journal of Rock Mechanics and Mining Sciences.* Vol. 26, no. 6, 613-627.

Wawersik, W.R., Carlson, L.W., Henfling, J.A., Borns, D.J., Beauheim, R.L., Howard, C.L., and Roberts, R.M. 1997. *Hydraulic Fracturing Tests in Anhydrite Interbeds in the WIPP, Marker Beds 139 and 140.* SAND95-0596. Albuquerque, NM: Sandia National Laboratories.

Information Only